Chapter-6

STUDIES ON SPECTRAL CHARACTERIZATION AND NUCLEASE ACTIVITY OF DINUCLEAR COPPER(II) AND NICKEL(II) COMPLEXES FORMED WITH TETRADENTATE LIGANDS CONTAINING POLYMETHYLENE GROUPS

Introduction

Transition metal complexes containing ***salen*** type of ligands derived from o-hydroxy aromatic carbonyl compound and various primary amines have been the subject of a number of investigations [1,3]. Condensation of o-hydroxy aromatic carbonyl compound with diamines in 2:1 molar ratio yields in the formation of tetradentate ligands. Studies on transition metal complexes derived from polymethylene ligands with varying chain length [3] are limited. Survey of literature reveals that DNA binding and cleavage activities of present complexes are not reported so for.

In the light of the above, several ***salen-type*** of ligands were synthesized by condensing salicylaldehyde/o-hydroxyacetophenone against polymethylene diamines with varying chain length. These ligands were characterized by physico-chemical properties, IR, ^{1}H-NMR, mass spectral and elemental analysis. The results are presented and discussed in Section 6.1. Binuclear copper(II) and nickel(II) complexes were synthesized and characterized by physico-chemical and spectral analysis. Electrochemical behavior of the complexes was investigated through cyclic voltammetric studies. Binding interactions with calf thymus DNA were carried out using absorption spectrophotometry. The results are discussed in Section 6.2. Cleavage activities of these complexes were investigated on a double stranded pBR plasmid DNA by using gel electrophoresis experiments in the absence and in the presence of an oxidant, a complexing agent, a free radical scavenger and a reducing agent. The observations are presented in Section 6.3.

Section 6.1: Characterization of ligands

Six ligands were prepared from salicylaldehyde/2-hydroxyacetophenone and 1,6-diaminohexane/ 1,7-diaminoheptane /1.8-diaminooctane in 2:1 molar ratio. Synthesis of ligands was given in Chapter 3, Section 3(ii). General structure of the ligands is given in Fig 6.1.1.

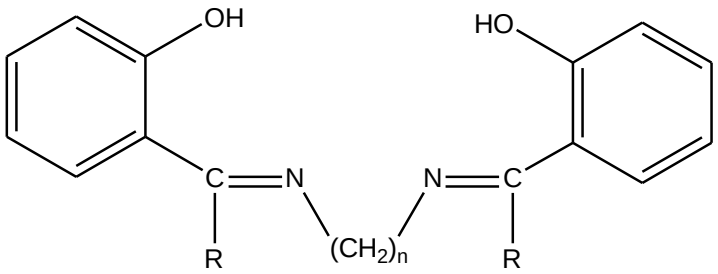

Where:	**R**	**n**	**Ligand**
	H	8	2,2'(1,8-diiminooctamethylene)methyl bis phenol (SALOCMN)
	H	7	2,2'(1,7-diiminoheptamethylene)methyl bis phenol (SALHPMN)
	H	6	2,2'(1,6-diiminohexamethylene)methyl bis phenol (SALHXMN)
	CH_3	8	2,2'(1,8-diiminooctamethylene)ethyl bis phenol (HAPOCMN)
	CH_3	7	2,2'(1,7-diiminoheptamethylene)ethyl bis phenol (HAPHPMN)
	CH_3	6	2,2'(1,6-diiminohexamethylene)ethyl bis phenol (HAPHXMN)

(i) Physico-chemical properties:

All the ligands were obtained as bright yellow crystalline products. All these are insoluble in water, sparingly soluble in methanol but readily soluble in DMF, CH_3CN, DMSO and chloroform. Melting points and elemental analysis data are given in **Table 6.1.1**.

Table 6.1.1: Analytical and physico-chemical data of ligands

Ligand	Mol. Formula	Mol. Weight	Colour (Yield)	Melting Point	Elemental analysis *		
					C%	H%	N%
SALOCMN	$C_{22}H_{28}N_2O_2$	352	Yellow (82%)	63-65°C	75.12 (74.97)	7.96 (8.01)	7.92 (7.95)
SALHPMN	$C_{21}H_{26}N_2O_2$	338	Yellow (87%)	45-47°C	74.23 (74.52)	7.92 (7.74)	8.21 (8.28)
SALHXMN	$C_{20}H_{24}N_2O_2$	324	Yellow (88%)	70-72°C	74.12 (74.04)	7.64 (7.46)	8.52 (8.64)
HAPOCMN	$C_{24}H_{32}N_2O_2$	380	Yellow (80%)	135-137°C	75.68 (75.75)	8.52 (8.48)	7.41 (7.36)
HAPHPMN	$C_{23}H_{30}N_2O_2$	366	Yellow (85%)	92-94°C	75.45 (75.37)	8.32 (8.25)	7.69 (7.64)
HAPHXMN	$C_{22}H_{28}N_2O_2$	352	Yellow (84%)	150-152°C	74.96 (74.97)	8.13 (8.01)	7.98 (7.95)

* Calculated values are given in the paranthesis

(ii) Infrared Spectral analysis

The infrared spectra of all the ligands were recorded in 4000-450 cm^{-1} region using KBr discs. Important IR spectral bands of the ligands and their tentative assignments are given in **Table 6.1.2**. Typical FT-IR spectrum of SALOCMN is shown in **Fig 6.1.1.**

Absence of vibrational band in the region 1740-1690 cm^{-1} indicates the absence of C=O group. Broad peak in the region 3344 – 3446 cm^{-1} is assigned to hydroxy group attached to phenyl ring. The decrease in phenolic ν(OH) is due to its involvement in *intramolecular* hydrogen bonding. Vibrational bands in the region 1603-1615 cm^{-1}suggest the presence of imine (>C=N) bond in Schiff base ligands. Vibration band in the region 742-764 cm^{-1} refers to $–CH_2-$ rocking [4].

Table 6.1.1: Important IR spectral bands and their tentative assignments

S.No.	Ligand	ν(OH)	ν(Ar C-H)	ν(C=N)	ν(C-O)	ν($-CH_2-$)
1.	SALOCMN	3354	2920	1603	1145	753
2.	SALHPMN	3378	2927	1615	1153	742
3.	SALHXMN	3384	2932	1612	1162	764
4.	HAPOCMN	3344	2836	1614	1150	744
5.	HAPHPMN	3346	2854	1614	1162	752
6.	HAPHXMN	3446	2859	1611	1157	761

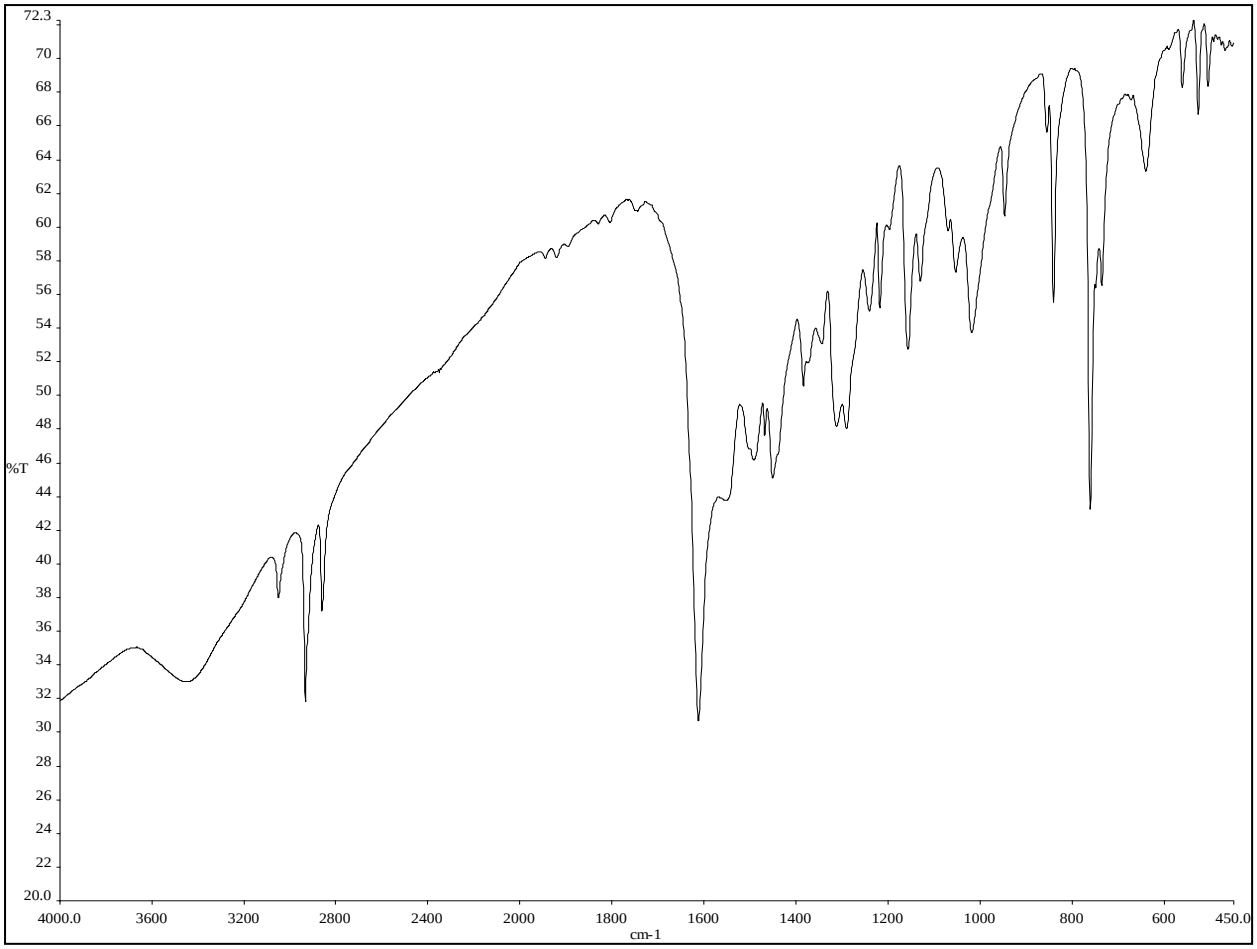

Fig 6.1.1: FT-IR spectrum of SALOCMN

(iii) ^{1}H-NMR spectra

The spectral data incorporating chemical shifts (δ), multiplicity and proton assignments are presented in **Table 6.1.3**. Typical ^{1}H-NMR spectrum of SALOCMN is shown in **Fig 6.1.2**. Sharp singlets at δ 8.0 - 8.4 are assigned to hydroxy protons. Broad multiplets centered between δ 6.7 and 7.5 observed in low field strength regions of spectra are due to ring protons. A triplet between δ 3.5 - 3.6 regions is due to methylene protons adjacent to imine nitrogen and multiplets between δ 1.4 - 1.7 are assigned to centre methylene groups. Singlets from δ 1.3 to 1.6 are assigned to methine protons. Singlets at δ 2.3 are assigned to methyl protons.

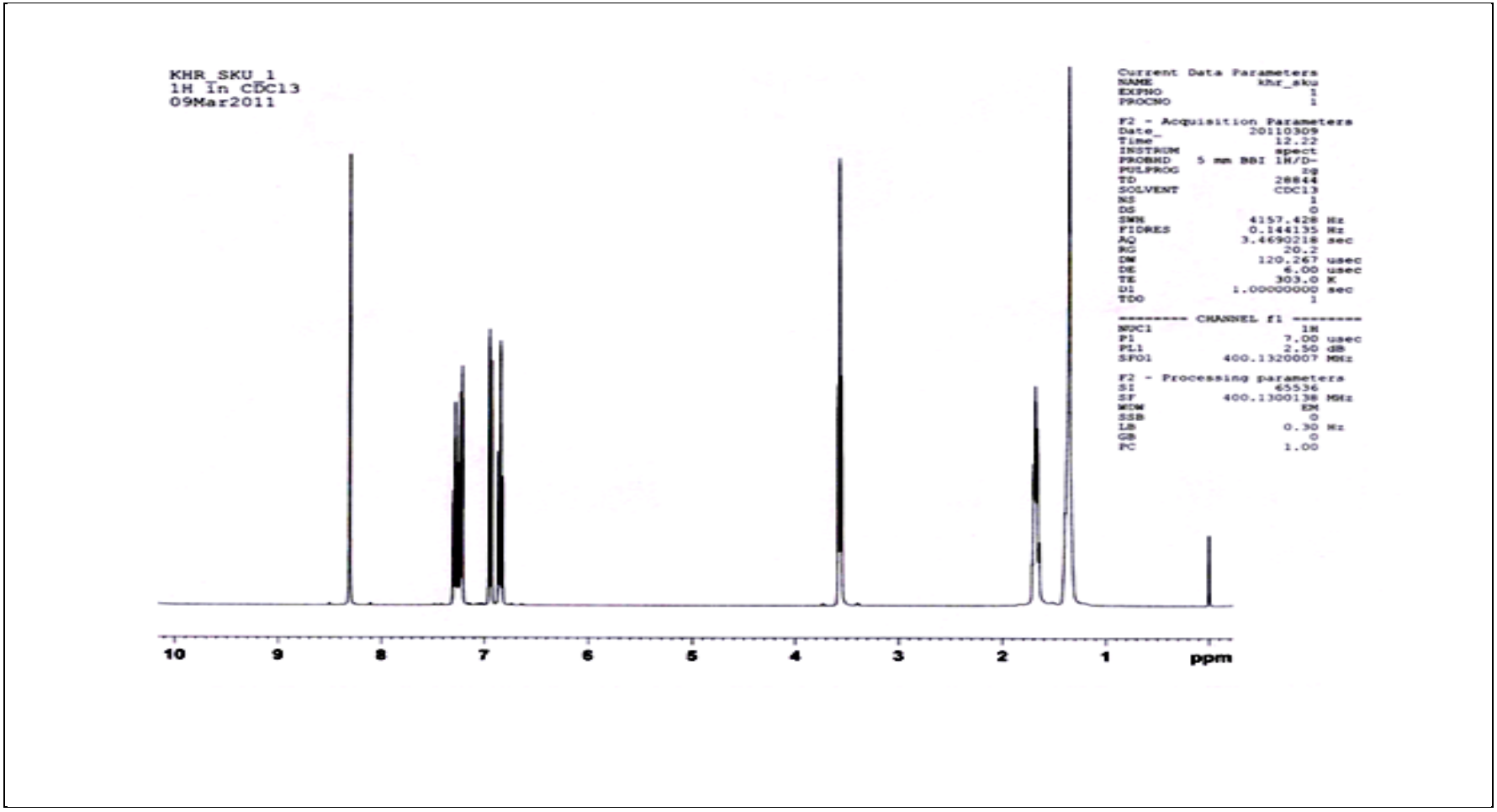

Fig 6.1.2: ^{1}H-NMR spectrum of SALOCMN

Table 6.1.3: ^{1}H-NMR spectral data of ligands

Ligand	Chemical shift (δ)	Multiplicity	No. of protons	Assignment
SALOCMN	8.2(s) 6.9-7.3(m) 3.5(s) 1.7(s) 1.3(s)	Singlet Multiplet Triplet Multiplet Singlet	2 8 4 12 2	O**H** Phenyl **H** -C**H**$_2$- -C**H**$_2$- =C**H**-
SALHPMN	8.2(s) 6.8-7.2(m) 3.6(s) 1.8(s) 1.6(s)	Singlet Multiplet Triplet Multiplet Singlet	2 8 4 8 2	O**H** Phenyl **H** -C**H**$_2$- -C**H**$_2$- =C**H**-
SALHXMN	8.4(s) 6.8-7.3(m) 3.6(s) 1.7(s) 1.4(s)	Singlet Multiplet Triplet Multiplet Singlet	2 8 4 10 2	O**H** Phenyl **H** -C**H**$_2$- -C**H**$_2$- =C**H**-
HAPOCMN	8.4(s) 7.2-7.5(m) 3.5(s) 2.3(s) 1.4-1.7(s)	Singlet Multiplet Triplet Singlet Multiplet	2 8 4 6 12	O**H** Phenyl **H** -C**H**$_2$- -C**H**$_3$ -C**H**$_2$-
HAPHPMN	8.0(s) 6.7-7.5(m) 3.5(s) 2.3(s) 1.4-1.7(s)	Singlet Multiplet Triplet Singlet Multiplet	2 8 4 6 10	O**H** Phenyl **H** -C**H**$_2$- -C**H**$_3$ -C**H**$_2$-
HAPHXMN	8.2(s) 6.7-7.5(m) 3.5(s) 2.3(s) 1.5-1.8(s)	Singlet Multiplet Triplet singlet Multiplet	2 8 4 6 8	O**H** Phenyl **H** -C**H**$_2$- -C**H**$_3$ -C**H**$_2$-

(iv) Mass spectra:

GC-MS Spectra of the ligands are recorded on JEOL GC MATE II GC-Mass spectrometer in EI^+ ionization mode. Mass spectrum of SALOCMN shows molecular ion peak at m/z 352 corresponding to its molecular weight. Mass spectra of SALHPMN, SALHXMN, HAPOCMN, HAPHPMN and HAPHXMN ligands show molecular ion peaks at m/z 338, 324, 380, 366 and 352 respectively corresponding to their molecular weights. Mass spectrum of SALOCMN is shown in **Fig 6.1.2**. General fragmentation pattern of the ligands are presented in Schemes 6.1.1, 6.1.2, 6.1.3, 6.1.4, 6.1.5 and 6.1.6 respectively. The percentage of abundance for different m/z values of ligands are given in **Tables 6.1.4 (a)** and **6.1.4 (b).**

Tables 6.1.4 (a): Mass spectral data of ligands

SALOCMN		**SALHPMN**		**SALHXMN**	
m/z value	% of Abundance	m/z value	% of Abundance	m/z value	% of Abundance
351	02	338	12	325	21
350	04	337	10	324	07
252	23	336	18	323	08
218	08	253	99	203	96
187	99	218	36	189	32
176	05	190	22	162	38
162	04	149	35	148	86
144	19	135	21	135	50
135	16	120	25	121	53
094	45	-	-	091	33

Tables 6.1.4 (b): Mass spectral data of ligands

HAPOCMN		**HAPHPMN**		**HAPHXMN**	
m/z value	% of Abundance	m/z value	% of Abundance	m/z value	% of Abundance
381	02	366	16	352	06
380	08	204	06	350	08
188	20	176	08	274	14
145	25	149	09	216	98
135	61	136	44	204	42
119	52	121	80	176	34
091	96	107	07	162	62
077	33	094	98	107	54
-	-	077	10	091	62

File: PRAGATI KHR-A Date Run: 03-08-2011 (Time Run: 15:24:34)
Sample:
Instrument: JEOL GCmate
Inlet: Direct Probe Ionization mode: EI+

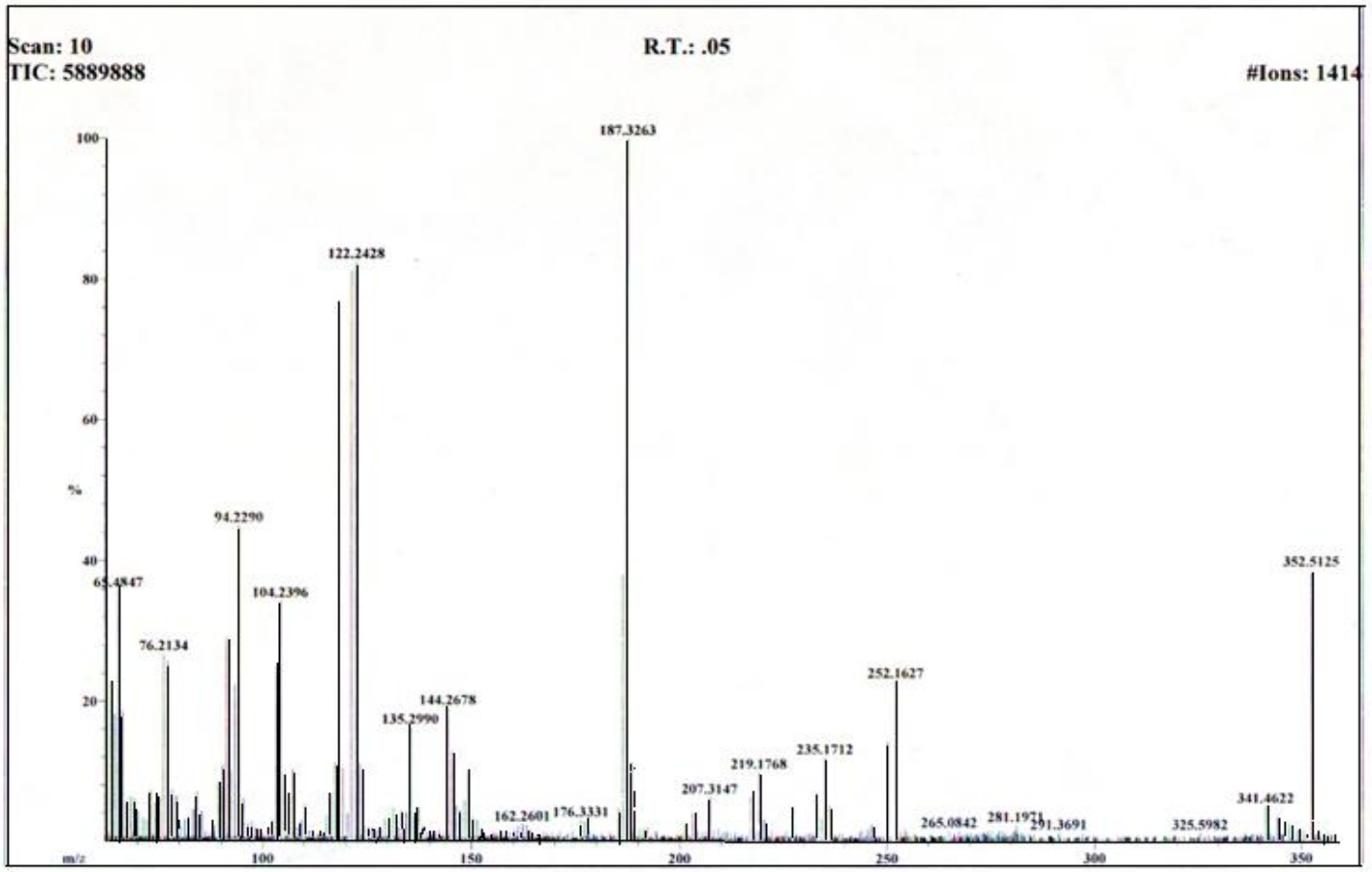

Fig 6.1.2: GC-MS spectrum of SALOCMN

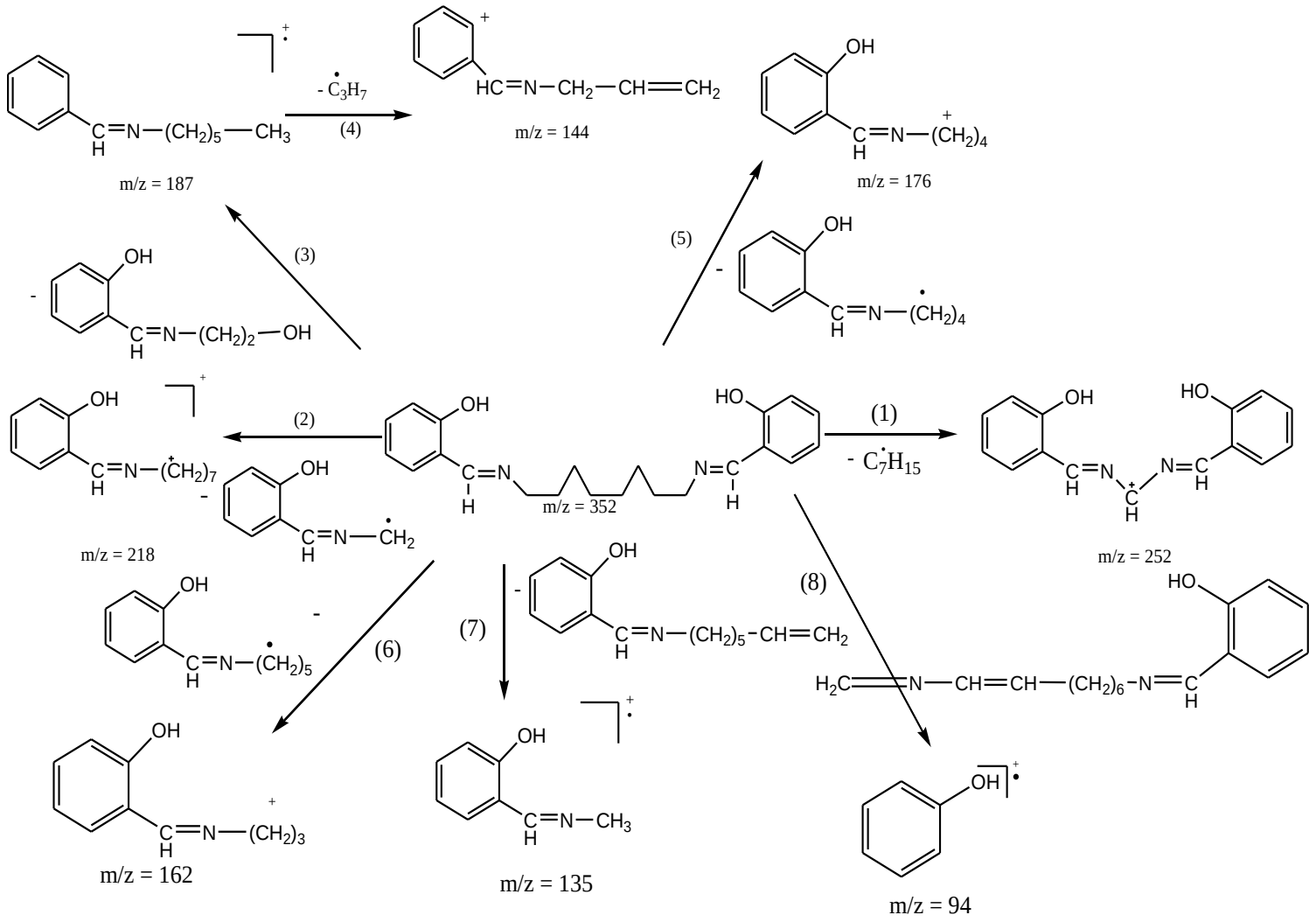

Scheme 6.1.1: Mass fragmentation pattern of SALOCMN

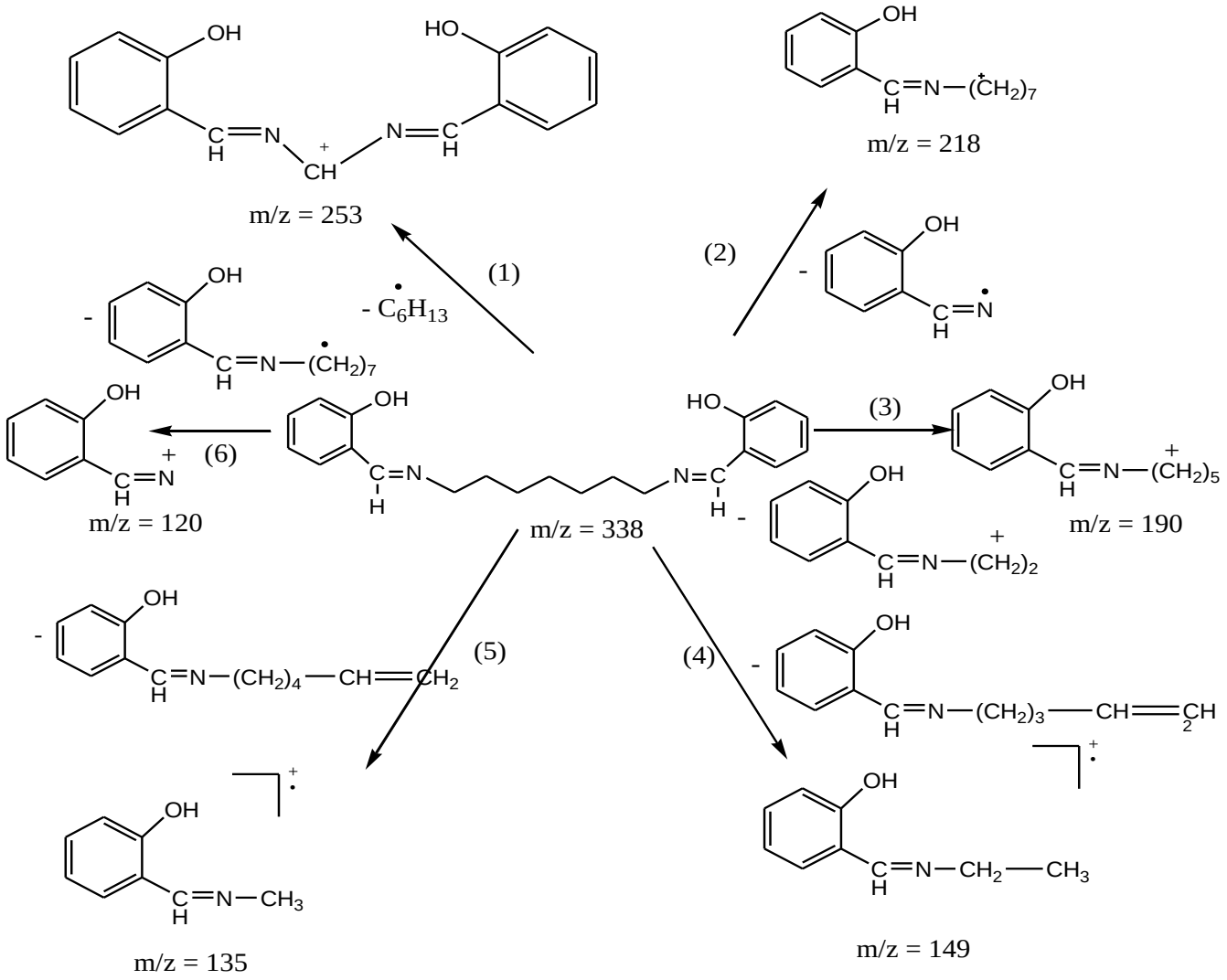

Scheme 6.1.2: Mass fragmentation pattern of SALHPMN

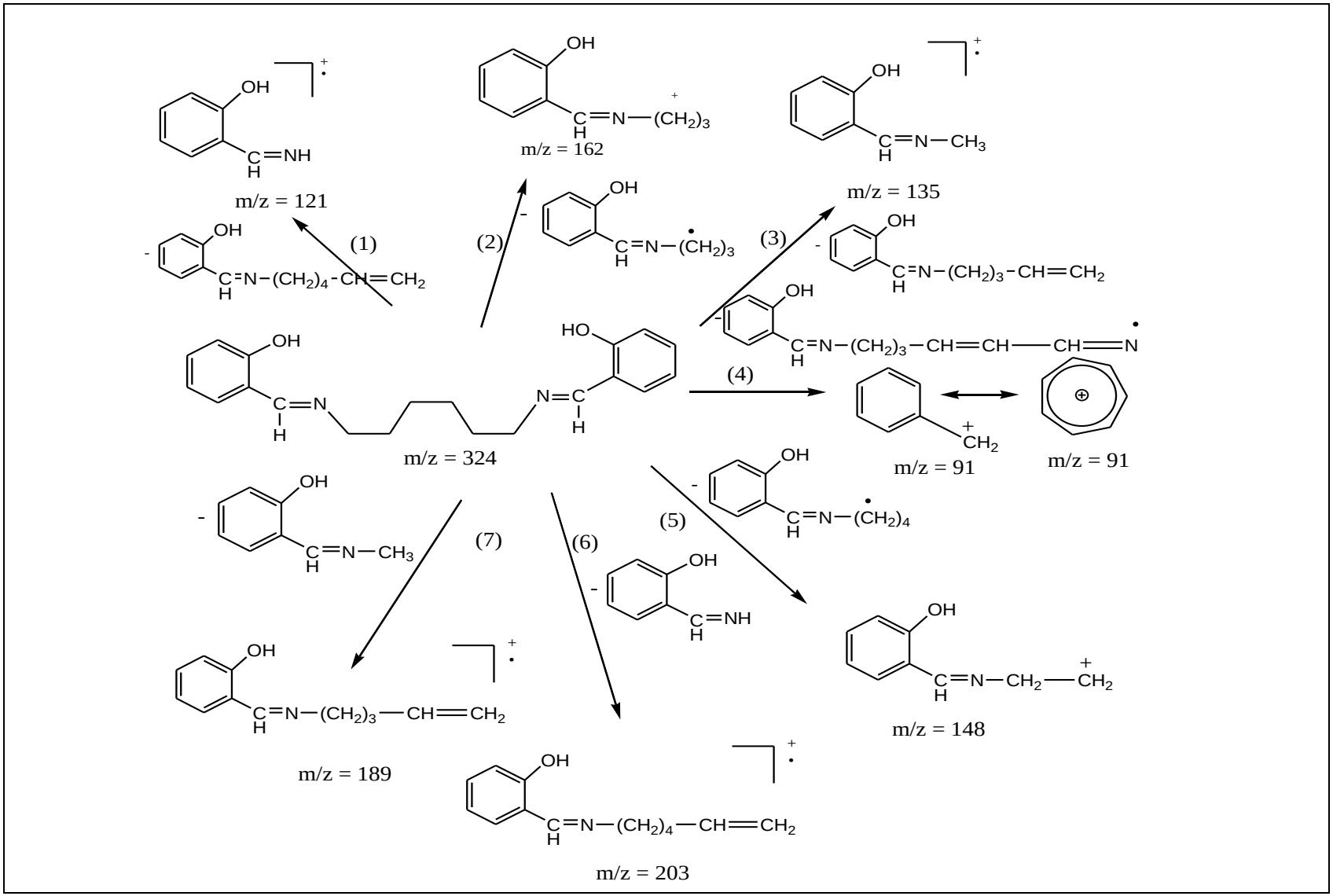

Scheme 6.1.3: Mass fragmentation pattern of SALHXMN

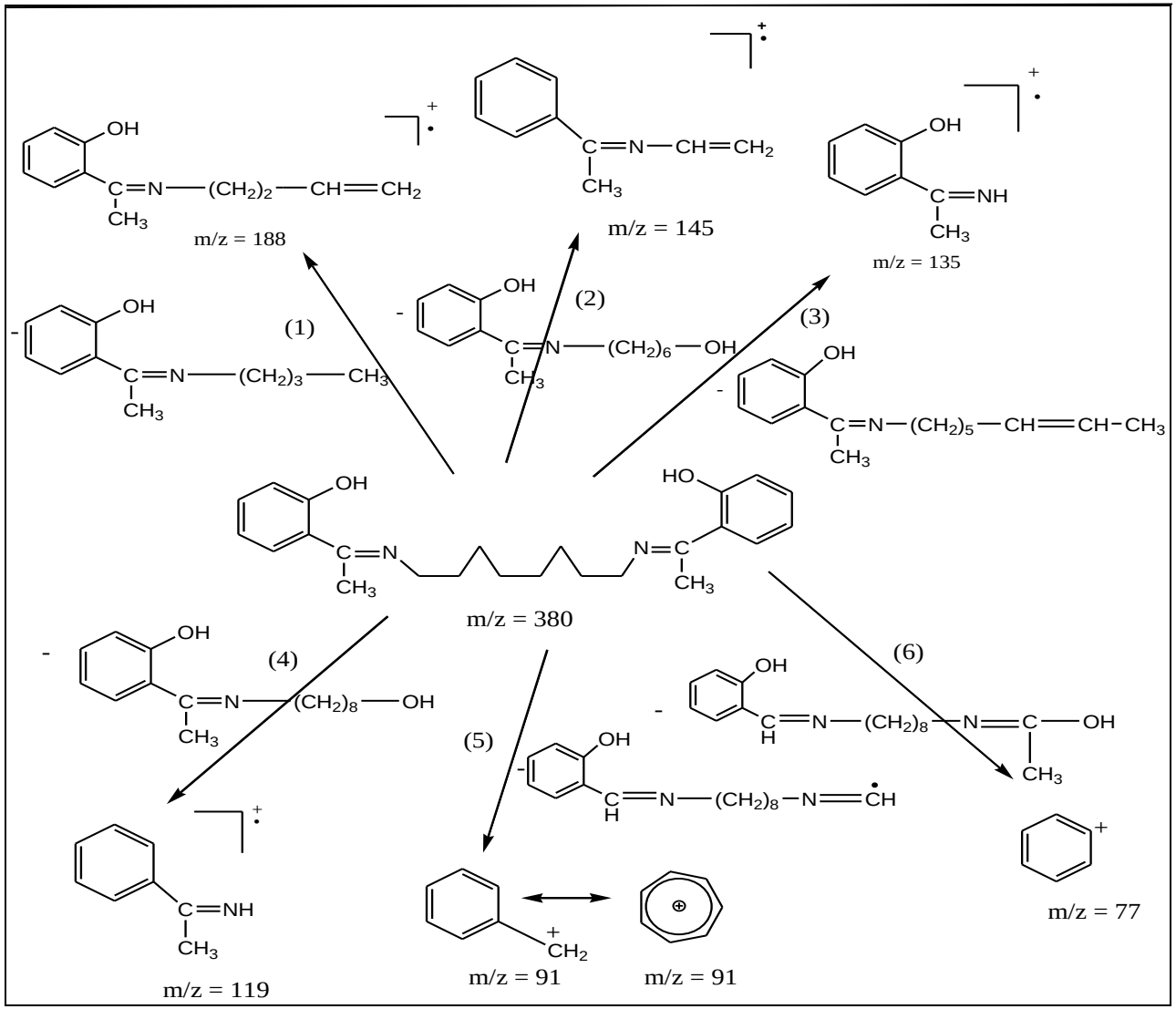

Scheme 6.1.4: Mass fragmentation pattern of HAPOCMN

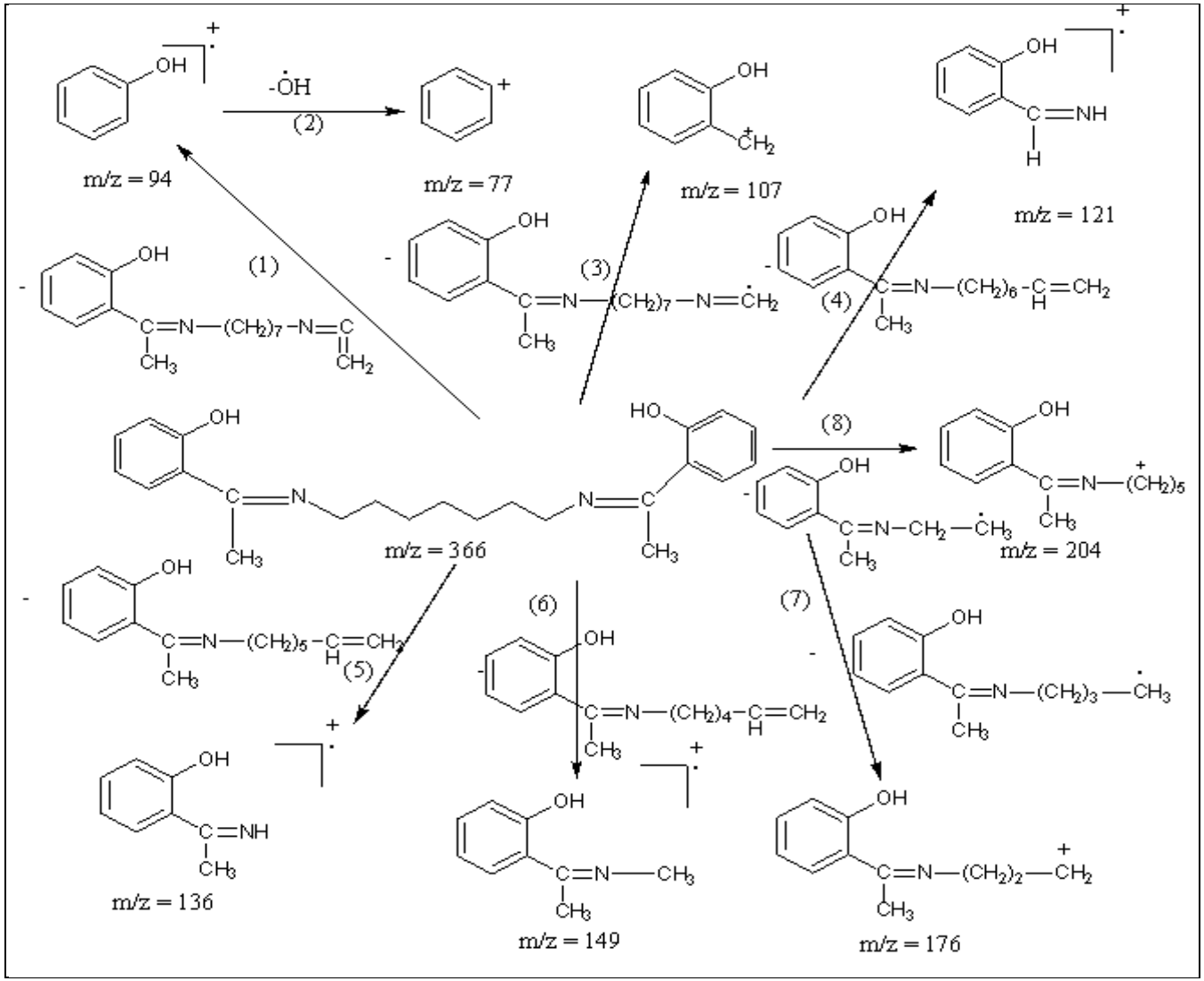

Scheme 6.1.5: Mass fragmentation pattern of HAPHPMN

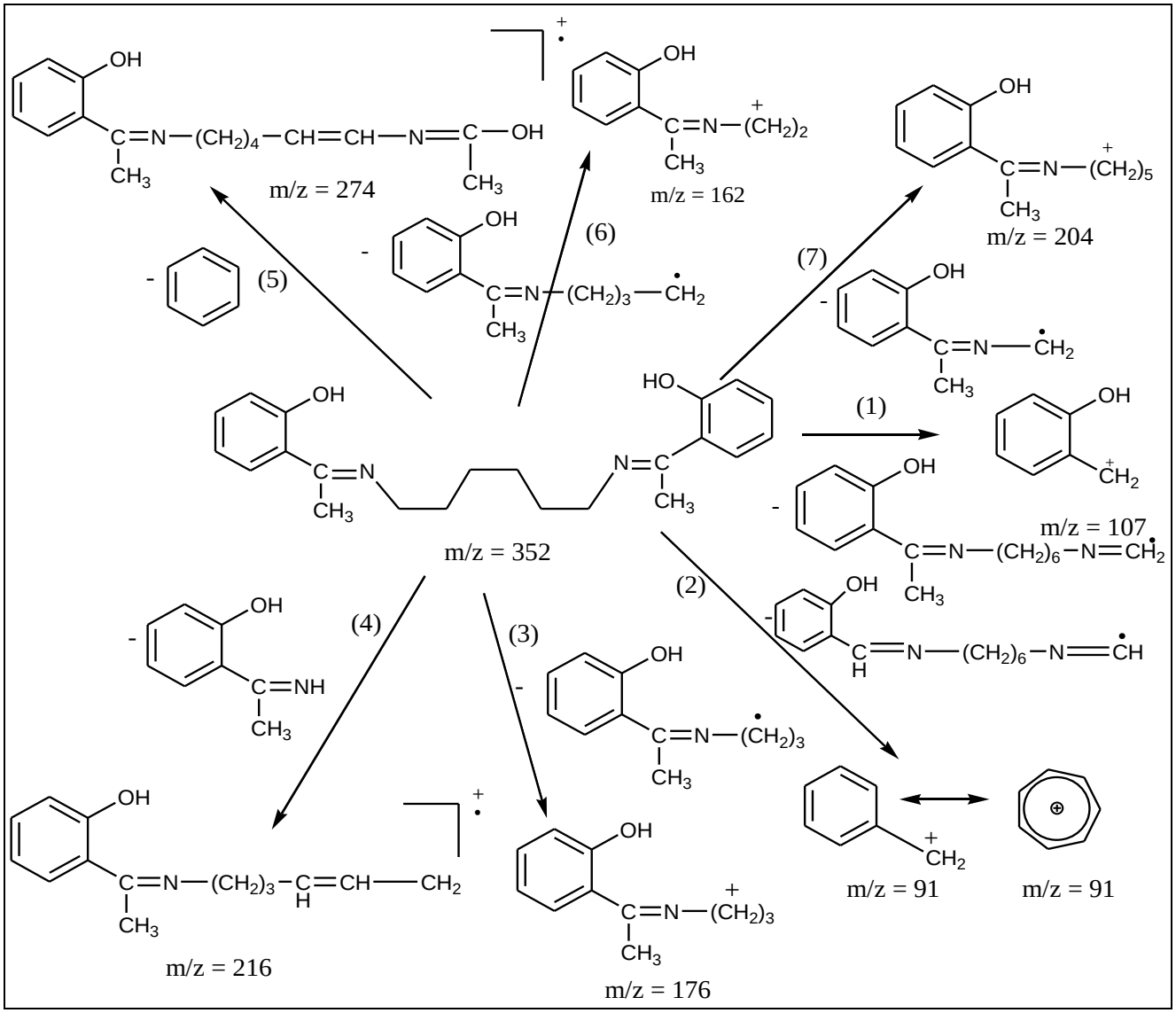

Scheme 6.1.6: Mass fragmentation pattern of HAPHXMN

Section 6.2: Characterization of metal complexes

Copper(II) and nickel(II) complexes of Schiff base ligands containing polymethylene groups are synthesized and characterized by employing physico-chemical and spectral methods. All the complexes are stable at room temperature, non-hygroscopic and non-volatile in nature. All the complexes are insoluble in water and methanol, but readily soluble in DMF and DMSO. Binding interactions with calf thymus DNA were carried out using absorption spectrophotometry. Cleavage activities of these complexes were investigated on a double stranded pBR plasmid DNA by using gel electrophoresis experiments in the absence and in the presence of an oxidant, a complexing agent, a free radical scavenger and a reducing agent.

(a) Conductivity measurements

Conductivity experiments were performed by dissolving the complexes in DMF at room temperature. Low molar conductivity values of present copper(II) and nickel II) complexes suggest non-electrolytic nature of the complexes [5]. The data are shown in **Table 6.2.1**.

(b) Magnetic moments

Magnetic susceptibility values of all the complexes were determined at 300K in solid state. The magnetic susceptibility data are presented in **Table 6.2.1.** The magnetic moment values of copper complexes are found to be sub-normal to spin only value [6-8]. The values are found to be in the range of 1.16 to 1.24 BM. The data reveal that these complexes are dimeric and there is strong metal-metal interaction between the two copper atoms. Nickel(II) complexes are found to be diamagnetic indicating the presence of square-planar geometry in solid state.

Table 6.2.1: Physico-chemical properties of metal complexes

S.No	Complex	Colour (Yield %)	Melting Point °C	Molar Conductance C_M ($\Omega^{-1}cm^{-2}mol^{-1}$)	μ_{eff} (BM)
1	$Cu_2(CH_3COO)_2(SALOCMN)_2$	Brownish green (48)	220-222*	9.26	1.21
2	$Ni_2(CH_3COO)_2(SALOCMN)_2$	Light green (38)	180-182	4.32	--
3	$Cu_2(CH_3COO)_2(SALHPMN)_2$	Brownish green (57)	> 300	10.34	1.24
4	$Ni_2(CH_3COO)_2(SALHPMN)_2$	Light green (47)	285-287*	3.28	--
5	$Cu_2(CH_3COO)_2(SALHXMN)_2$	Brownish green (50)	270-272*	9.85	1.18
6	$Ni_2(CH_3COO)_2(SALHXMN)_2$	Pale green (40)	> 300	03.26	--
7	$Cu_2(CH_3COO)_2(HAPOCMN)_2$	Orange red (46)	> 300	09.98	1.19
8	$Ni_2(CH_3COO)_2(HAPOCMN)_2$	Light green (46)	> 300	4.47	--
9	$Cu_2(CH_3COO)_2(HAPHPMN)_2$	Brownish green (46)	252-254*	11.22	1.22
10	$Ni_2(CH_3COO)_2(HAPHPMN)_2$	Pale green (46)	> 300	4.58	--
11	$Cu_2(CH_3COO)_2(HAPHXMN)_2$	Brownish green (51)	237-239*	10.44	1.16
12	$Ni_2(CH_3COO)_2(HAPHXMN)_2$	Light green (41)	> 300	4.92	--

* Decomposition temperature.

(c) Mass spectra:

LC-MS spectra of Cu(II) and Ni(II) complexes were recorded in DMF. The LC-MS spectrum of complex VII is shown in **Fig 6.2.1**. The spectrum shows peak at m/z = 623.39 (cal 623.08) represents the molecular ion peak of the complex. Calculated and found molecular weights of the complexes are given in **Table 6.2.2.**

Table 6.2.2: Mass spectral and elemental analysis of Cu(II) and Ni(II) complexes

Complex	Molecular formula	Mol. Weight*	Elemental analysis			
			C %	H %	N %	Cu/Ni %
$Cu_2(CH_3COO)_2(SALOCMN)_2$	$Cu_2(CH_3COO)_2C_{22}H_{26}N_2O_2$	595.16 (595.08)	52.47 (52.43)	5.36 (5.42)	4.76 (4.70)	21.33 (21.34)
$Ni_2(CH_3COO)_2(SALOCMN)_2$	$Ni_2(CH_3COO)_2C_{22}H_{26}N_2O_2$	585.67 (585.42)	52.95 (52.43)	5.56 (5.42)	4.72 (4.70)	20.35 (21.34)
$Cu_2(CH_3COO)_2(SALHPMN)_2$	$Cu_2(CH_3COO)_2C_{21}H_{24}N_2O_2$	580.86 (581.08)	51.84 (51.63)	5.44 (5.20)	4.66 (4.82)	21.68 (21.85)
$Ni_2(CH_3COO)_2(SALHPMN)_2$	$Ni_2(CH_3COO)_2C_{21}H_{24}N_2O_2$	571.23 (571.42)	52.39 (51.63)	5.69 (5.20)	4.82 (4.80)	20.28 (21.85)
$Cu_2(CH_3COO)_2(SALHXMN)_2$	$Cu_2(CH_3COO)_2C_{20}H_{22}N_2O_2$	566.92 (567.08)	51.55 (51.67)	5.12 (5.06)	4.98 (5.02)	21.10 (21.04)
$Ni_2(CH_3COO)_2(SALHXMN)_2$	$Ni_2(CH_3COO)_2C_{20}H_{22}N_2O_2$	557.36 (557.42)	51.69 (51.67)	5.14 (5.06)	5.14 (5.02)	20.85 (21.04)
$Cu_2(CH_3COO)_2(HAPOCMN)_2$	$Cu_2(CH_3COO)_2C_{24}H_{30}N_2O_2$	623.38 (623.08)	54.12 (53.92)	5.76 (5.82)	4.58 (4.49)	20.09 (20.38)
$Ni_2(CH_3COO)_2(HAPOCMN)_2$	$Ni_2(CH_3COO)_2C_{24}H_{30}N_2O_2$	612.86 (613.42)	54.06 (53.92)	5.92 (5.82)	4.44 (4.49)	20.22 (20.38)
$Cu_2(CH_3COO)_2(HAPHPMN)_2$	$Cu_2(CH_3COO)_2C_{23}H_{28}N_2O_2$	609.29 (609.08)	53.22 (53.19)	5.68 (5.62)	4.46 (4.59)	20.82 (20.85)
$Ni_2(CH_3COO)_2(HAPHPMN)_2$	$Ni_2(CH_3COO)_2C_{23}H_{28}N_2O_2$	600.33 (599.42)	53.13 (53.19)	5.79 (5.62)	4.44 (4.59)	20.94 (20.85)
$Cu_2(CH_3COO)_2(HAPHXMN)_2$	$Cu_2(CH_3COO)_2C_{22}H_{26}N_2O_2$	595.58 (595.08)	51.55 (52.43)	5.56 (5.42)	4.99 (4.70)	21.92 (21.34)
$Ni_2(CH_3COO)_2(HAPHXMN)_2$	$Ni_2(CH_3COO)_2C_{22}H_{26}N_2O_2$	586.06 (585.42)	52.26 (52.43)	5.38 (5.42)	4.72 (4.70)	21.38 (21.34)

Calculated values are given in parentheses

*Determined using LC-MS

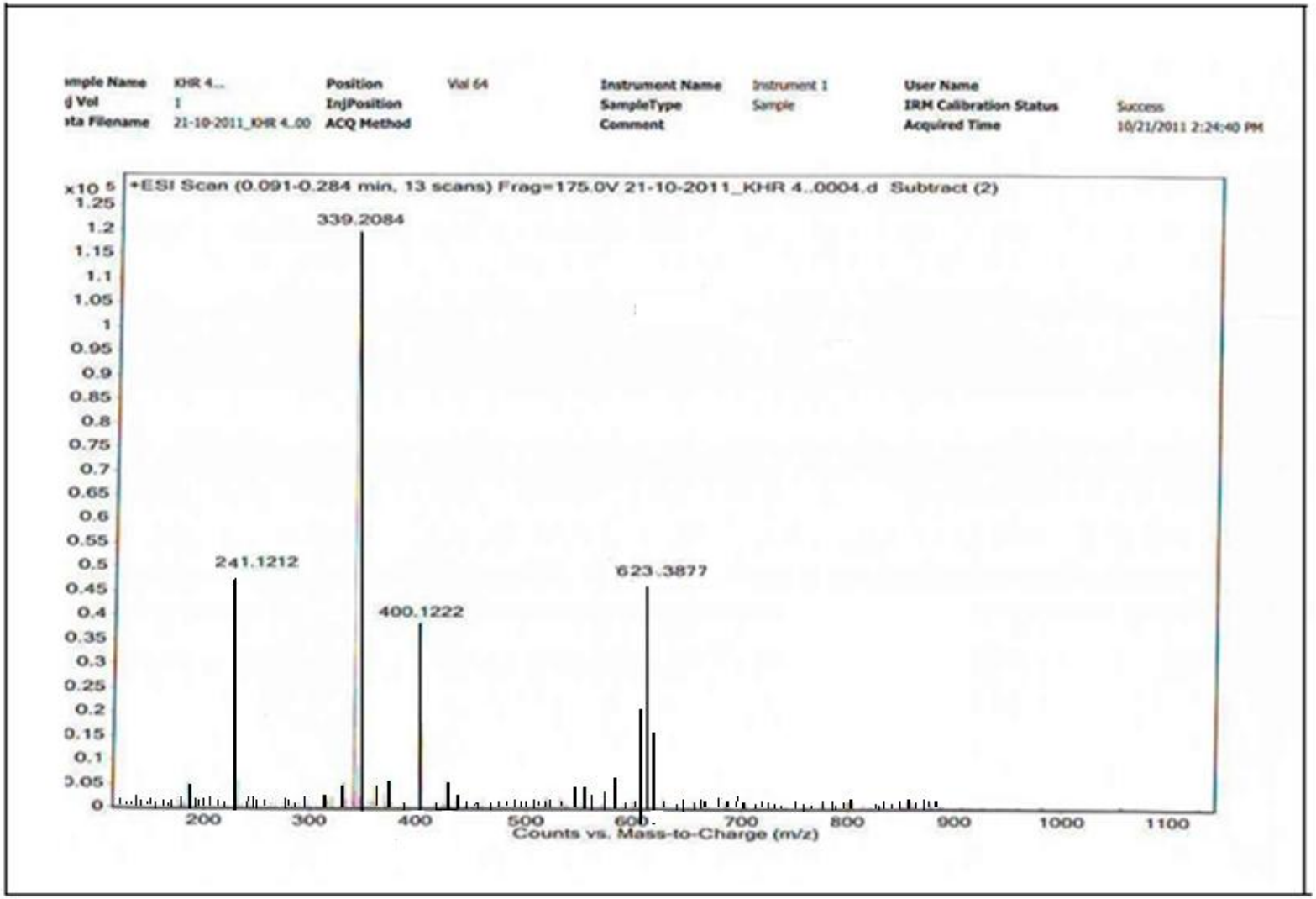

Fig 6.2.1: LC-MS spectrum of $Cu_2(CH_3COO)_2(HAPOCMN)_2$

(d) Electronic spectral data:

Electronic absorption spectra of copper(II) and nickel(II) complexes were recorded in DMF. All the complexes show high intensity bands in the region 32894-32467 cm^{-1} due to intra-ligand transition. The bands in the 27186-27262 cm^{-1} region are assigned to metal to ligand charge transfer transition (M→L CT). Typical electronic spectrum of $Cu_2(CH_3COO)_2(SALHXMN)_2$ is shown in **Fig 6.2.2**. Low intensity broad structured band in the 15878-15996 cm^{-1} region is assigned to d-d transition. Electronic spectral data copper(II) complexes are given in **Table 6.2.3(a).** There is a gradual increase in the d-d transition energy value as the length of the polymethylene chain decreases from 8 to 6.

Table 6.2.3 (a):

Electronic spectral data (cm^{-1}) of copper(II) complexes in DMF medium

Complex	$\pi - \pi^*$	Charge transfer (M→L CT)	d-d transition
$Cu_2(CH_3COO)_2(SALOCMN)_2$	32894	27100	15748
$Cu_2(CH_3COO)_2(SALHPMN)_2$	32573	27247	15873
$Cu_2(CH_3COO)_2(SALHXMN)_2$	32786	27472	15974
$Cu_2(CH_3COO)_2(HAPOCMN)_2$	32679	27322	15576
$Cu_2(CH_3COO)_2(HAPHPMN)_2$	32894	27624	15822
$Cu_2(CH_3COO)_2(HAPHXMN)_2$	32467	27932	15923

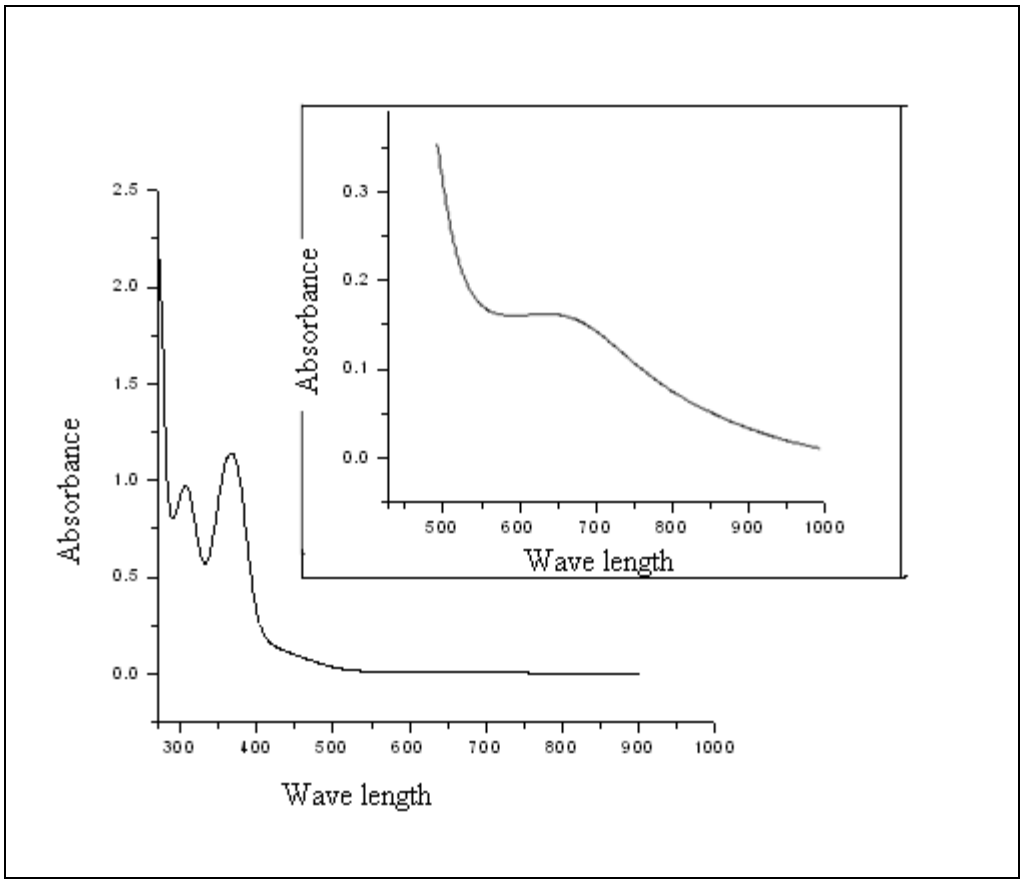

Fig 6.2.2: Electronic spectrum of $Cu_2(CH_3COO)_2(SALHXMN)_2$; spectrum of highly concentrated solution is given in the inset

Three transition bands are observed in the spectra of nickel complexes in 11402-11494 cm^{-1} (ν_1 - peak a in Fig 6.2.3-B), 15600-15898 cm^{-1} (ν_2 - peak b in Fig 6.2.3-A) and 30303- 30864 cm^{-1} (ν_3 - peak a in Fig 6.2.3-A) from low energy to high energy. These bands are assigned to $^3A_{2g}(F) \rightarrow {}^3T_{2g}(\nu_1)$, $^3A_{2g}(F) \rightarrow {}^3T_{1g}(\nu_2)$ and $^3A_{2g}(F) \rightarrow {}^3T_{1g}(P)(\nu_3)$, which clearly indicates octahedral stereochemistry of the complexes in DMF medium. Spectral data have been utilized to compute important ligand field parameters (10Dq) and B') using the ligand field of spin allowed transitions in d^8 configuration. Electronic spectral data and ligand field parameters of nickel complexes are given in **Table 6.2.3(b).** Comparison of 10 Dq and Racah interelectronic repulsion parameter (B') values for nickel complexes indicates that the ligands give reasonably strong covalent bonds. The ligand field parameters are

consistent with the coordination of azomethine nitrogen. The (ν_2)/ (ν_1) ratio lies between 1.45-1.52 range as expected for octahedral nickel(II) complexes. Using Figgi's equation, $\Delta_o = f \, x \, g$ and by substituting g factor (8700 cm^{-1}) which is characteristic metal field strength of ligand (f) values are calculated. The ***f*** values are between 1.39-1.43. The LFSE values of these complexes are nearly the same and reflect the presence of identical coordination around the central metal ion. It may be suggested that hexacoordination of metal is felicitated by axial coordination of solvent. Typical electronic spectrum of $Ni_2(CH_3COO)_2(SALHXMN)_2$ is shown in **Fig 6.2.3**.

Table 6.2.3(b): Electronic spectral data of nickel (II) complexes

Complex	ν_1	ν_2	ν_3	B’	β	10 Dq	$\nu_2 - \nu_1$	ν_2/ν_1	LFSE	*f*
$Ni_2(CH_3COO)_2(SALOCMN)_2$	11402	15600	30303	780	0.74	11402	4198	1.36	32.57	1.310
$Ni_2(CH_3COO)_2(SALHPMN)_2$	11441	15797	30303	785	0.75	11441	4356	1.38	32.68	1.315
$Ni_2(CH_3COO)_2(SALHXMN)_2$	11494	15873	30674	804	0.76	11494	4379	1.38	32.84	1.321
$Ni_2(CH_3COO)_2(HAPOCMN)_2$	11428	15673	30581	798	0.76	11428	4245	1.37	32.65	1.313
$Ni_2(CH_3COO)_2(HAPHPMN)_2$	11494	15822	30769	807	0.77	11494	4328	1.37	32.84	1.321
$Ni_2(CH_3COO)_2(HAPHXMN)_2$	11520	15898	30864	813	0.77	11520	4378	1.38	32.91	1.324

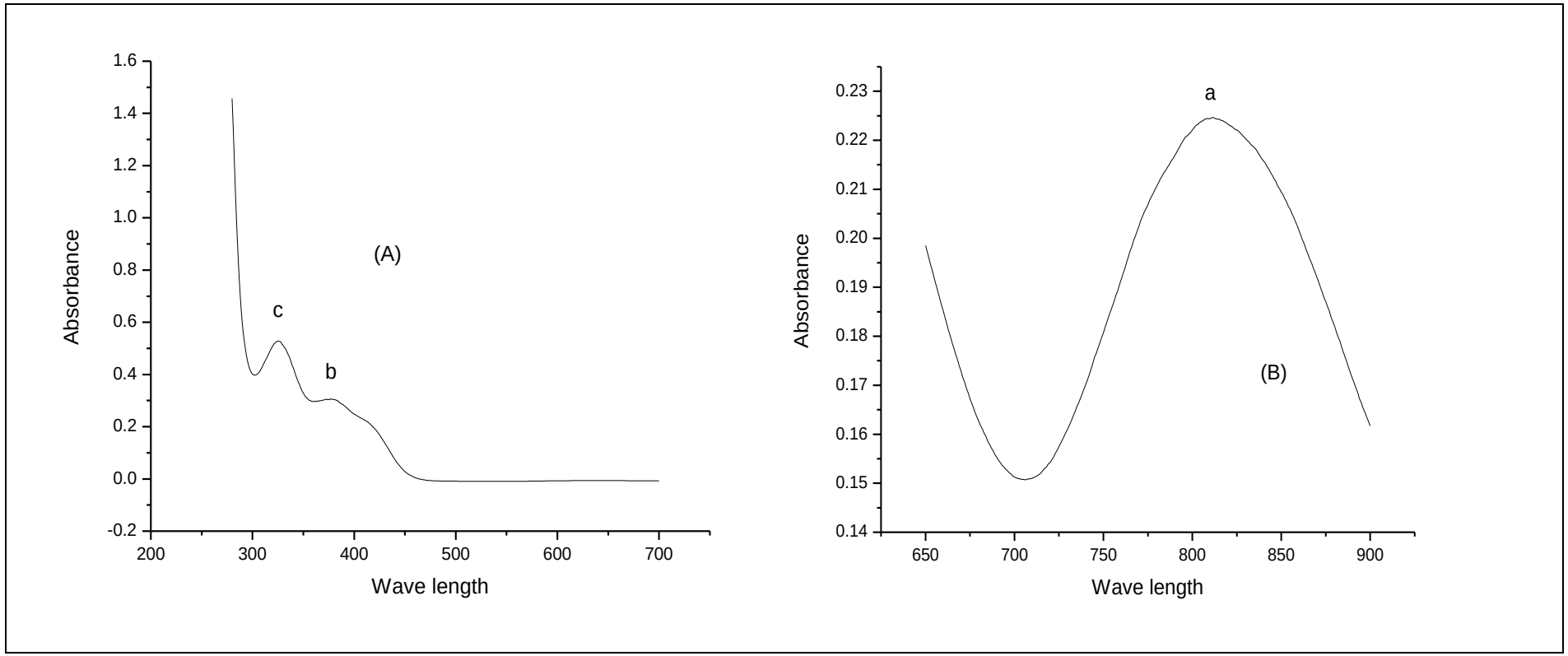

Fig 6.2.3: (A) Electronic spectrum of $Ni_2(CH_3COO)_2(SALHXMN)_2$; (B) spectrum of highly concentrated solution; a, b and c represent ν_1, ν_2 and ν_3 respectively.

(e) Infrared spectral studies:

Infrared spectra of copper(II) and nickel (II) complexes are compared with ligand spectra. Typical IR spectrum of $Cu_2(CH_3COO)_2(SALHXMN)_2$ is shown in **Fig 6.2.4.** Important IR spectral bands of complexes are presented in **Table 6.2.4**. The donor sites of ligands have been identified from infrared spectral studies. The ν (OH) stretching vibration is observed at 3344-3446 cm^{-1} in ligands, this absorption band is absent in complexes suggesting the deprotonation of –OH in complex formation. The C=N (imine) vibration is observed in 1603-1615 cm^{-1} range in the IR spectra of ligands. This band is shifted to lower wave number in IR spectra of all the complexes suggesting the participation of azomethine nitrogen atom in coordination with metal atom [9]. The strong bands observed in 1542-1575 cm^{-1} region are due to the presence of bridging acetato group [10,11]. Stretching vibrations of free acetate ion occurs in the range 1115-1160 cm^{-1} whereas the terminal acetate causes vibrational peak in the region 1040-1060 cm^{-1} [12]. The lowering of the position of the phenolic C-O bands in the complexes indicates the formation of covalent bond between metal and oxygen [13]. In the IR spectra of all the complexes aromatic ring vibrations and C=C vibrations are not much affected. The non-ligand absorption bands occurring in the regions 508-568 cm^{-1} and 411-474 cm^{-1} are assigned to $\nu_{(M-O)}$ and $\nu_{(M-N)}$ respectively [14].

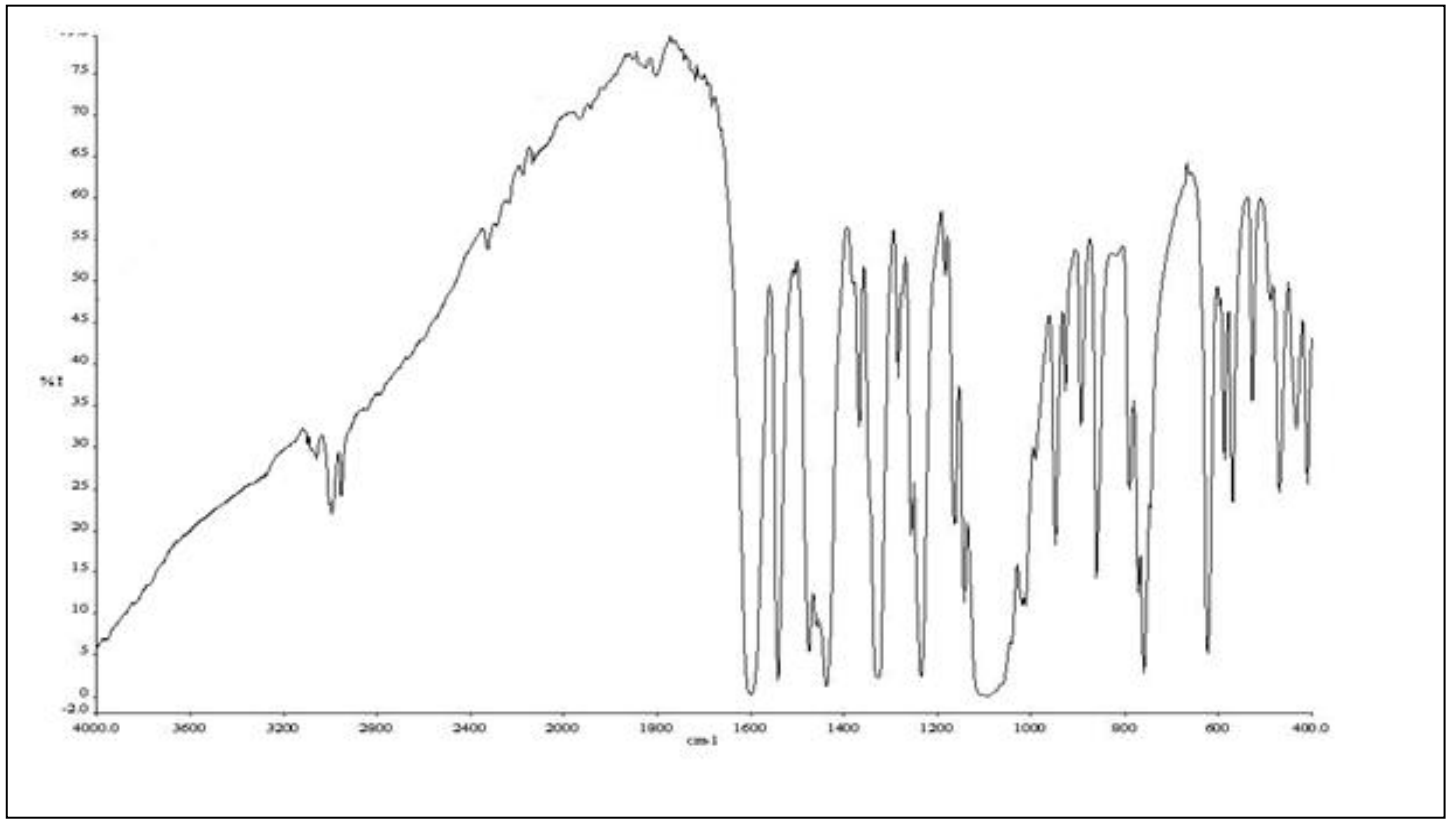

Fig 6.2.4: FT-IR spectrum of $Cu_2(CH_3COO)_2(SALHXMN)_2$

Table 6.2.4: **Important IR spectral bands of metal complexes and their assignments**

Ligand/ Complex	ν (Ar CH) cm^{-1}	ν (C=N) cm^{-1}	ν (acetate) cm^{-1}	ν(C-O) cm^{-1}	(M-O) cm^{-1}	(M-N) cm^{-1}
SALOCMN	2920	1603	--	1145	--	--
$Cu_2(CH_3COO)_2(SALOCMN)_2$	2920	1600	1554	1142	518	423
$Ni_2(CH_3COO)_2(SALOCMN)_2$	2920	1601	1548	1140	563	474
SALHPMN	2927	1615	--	1153	--	--
$Cu_2(CH_3COO)_2(SALHPMN)_2$	2927	1611	1572	1152	509	428
$Ni_2(CH_3COO)_2(SALHPMN)_2$	2927	1612	1556	1150	558	467
SALHXMN	2932	1612	--	1162	--	--
$Cu_2(CH_3COO)_2(SALHXMN)_2$	2932	1609	1575	1160	512	416
$Ni_2(CH_3COO)_2(SALHXMN)_2$	2932	1610	1570	1160	566	467
HAPOCMN	2886	1614	--	1150	--	--
$Cu_2(CH_3COO)_2(HAPOCMN)_2$	2886	1612	1565	1148	518	416
$Ni_2(CH_3COO)_2(HAPOCMN)_2$	2886	1611	1546	1149	568	439
HAPHPMN	2854	1614	--	1162	--	--
$Cu_2(CH_3COO)_2(HAPHPMN)_2$	2854	1612	1548	1160	506	411
$Ni_2(CH_3COO)_2(HAPHPMN)_2$	2854	1613	1542	1160	550	449
HAPHXMN	2859	1611	--	1157	--	--
$Cu_2(CH_3COO)_2(HAPHXMN)_2$	2859	1609	1559	1154	512	414
$Ni_2(CH_3COO)_2(HAPHXMN)_2$	2859	1610	1552	1155	558	439

(f) ESR spectral studies:

ESR spectra of copper complexes were recorded at room temperature and liquid nitrogen temperature (LNT) in both solution ((DMF) and solid state.

The spin Hamiltonian and orbital reduction parameters of copper complexes are given in **Tables 6.2.5(a)** and **6.2.5(b).** The g∥ and g ⊥ values are computed from the spectrum using tetracyanoethylene (TCNE) free radical as 'g' marker. Kivelson and Neiman [15] have reported that g∥ value is less than 2.3 for covalent character and is greater than 2.3 for ionic character of the metal ligand bond in complexes. It is significant from the data that the observed g∥ values for all these copper complexes are less than 2.3 suggesting covalent character of the metal-ligand bonding. The g tensor values of copper(II) complexes can be used to derive the ground state. In square planar complexes, unpaired electron lies in the $d_{x^2-y^2}$ orbitals giving $^2B_{1g}$ as the ground state with g∥ > g ⊥ >2.0023, while the unpaired electron lies in the d_{z^2} orbital giving $^2A_{1g}$ as the ground state with g ⊥ > g∥ > 2.0023. From the observed values of complexes at 300K and 77K in solid state spectrum it is clear that g∥ > g ⊥ >2.0023 which suggests the fact that the unpaired electron lies predominantly in the $d_{x^2-y^2}$ orbital [16]. The g_{av} value for these complexes is greater than 2 indicating covalent nature of the metal-ligand bond [17].

In the solid state, similar spectra of these complexes at 77K and 300K indicates that the geometry around copper (II) ion is unaffected on cooling to liquid nitrogen temperature. In these conditions the axial symmetry parameter G, which measures the interaction between copper centres in unit cell is calculated from the following equation [18].

$$G = [g_{\parallel} - 2.0023 / g_{\perp} - 2.0023]$$

The calculated G values are found to be less than 4 for all the copper complexes suggesting that there are considerable interactions between metal ions in the solid complex [19].

ESR spectra were recorded in DMF at room temperature and liquid nitrogen temperature to obtain more accurate molecular values by giving four hyperfine signals for all the complexes. Typical ESR spectra of $Cu_2(CH_3COO)_2(HAPHPMN)_2$ in powder state at 300K, at Liquid Nitrogen Temperature, in DMF solution at 300K and at liquid nitrogen temperature are shown in **Fig 6.2.5.**

The ESR parameters ($g_\parallel$, $g_\perp$, $A_\parallel$, $A_\perp$)of the complexes and the energies of d-d transitions are used [20-23] to evaluate spin-orbit coupling constant (λ) and the orbital reduction parameters ($K_\parallel$, $K_\perp$). The trend $g_\parallel > g_\perp > g_e$ (2.0023) observed for these complexes suggests that the unpaired electron is localized in $d_{x^2-y^2}$ orbital [24] of the copper (II) ion. For all the complexes the lowest g value greater than 2.0023 is also consistent with a $d_{x^2-y^2}$ ground state. The spin-orbit coupling constant (**λ**) value is calculated using the relation, $g_{av} = (g_\parallel + 2\, g_\perp)\, 1/3$ and $g_{av} = 2(1-2\, \lambda/10Dq)$, is less than the free copper(II) (832 cm^{-1}) which also supports covalent character of M-L bond. Hathaway [23] has pointed out that for the pure σ – bonding $K_\parallel \approx K_\perp \approx 0.77$, for in- plane π-bonding $K_\parallel > K_\perp$, while for out-of-plane π-bonding $K_\parallel < K_\perp$. The observed $K_\parallel < K_\perp$ relation in all the complexes indicates the presence of in-plane π-bonding [25].

Table 6.2.5(a): The spin Hamiltonian and orbital reduction parameters of copper complexes in powder state

Complex	At room temperature				At liquid nitrogen temperature(LNT)			
	$g_{\parallel}$	$g_{\perp}$	g_{av}	G	$g_{\parallel}$	$g_{\perp}$	g_{av}	G
$Cu_2(CH_3COO)_2(SALOCMN)_2$	2.214	2.177	2.189	1.210	2.217	2.181	2.193	1.201
$Cu_2(CH_3COO)_2(SALHPMN)_2$	2.148	2.113	2.124	1.318	2.148	2.113	2.124	1.315
$Cu_2(CH_3COO)_2(SALHXMN)_2$	2.152	2.092	2.112	1.661	2.143	2.092	2.109	1.559
$Cu_2(CH_3COO)_2(HAPOCMN)_2$	2.111	2.098	2.135	2.18	2.212	2.096	2.134	2.237
$Cu_2(CH_3COO)_2(HAPHPMN)_2$	2.214	2.093	2.133	2.334	2.214	2.093	2.133	2.334
$Cu_2(CH_3COO)_2(HAPHXMN)_2$	2.140	2.057	2.085	2.482	2.138	2.054	2.082	2.602

Table 6.2.5(b): The spin Hamiltonian and orbital reduction parameters of copper complexes in DMF solution

Complex	$g_{\parallel}$	$g_{\perp}$	g(av)	G	λ	$K_{\parallel}$	$K_{\perp}$	$A_{\parallel}$ cm^{-1}	$A_{\perp}$ cm^{-1}	A_{av}
$Cu_2(CH_3COO)_2(SALOCMN)_2$	2.106	2.052	2.070	2.086	276	0.860	1.191	0.153	0.072	0.099
$Cu_2(CH_3COO)_2(SALHPMN)_2$	2.129	2.066	2.087	1.989	345	0.854	1.211	0.065	0.025	0.039
$Cu_2(CH_3COO)_2(SALHXMN)_2$	2.125	2.075	2.091	1.690	363	0.822	1.265	0.065	0.019	0.034
$Cu_2(CH_3COO)_2(HAPOCMN)_2$	2.180	2.095	2.120	1.916	702	0.703	1.014	0.104	0.047	0.066
$Cu_2(CH_3COO)_2(HAPHPMN)_2$	2.126	2.064	2.084	2.014	332	0.858	1.212	0.065	0.022	0.036
$Cu_2(CH_3COO)_2(HAPHXMN)_2$	2.198	2.112	2.140	1.789	559	0.836	1.251	0.131	0.061	0.084

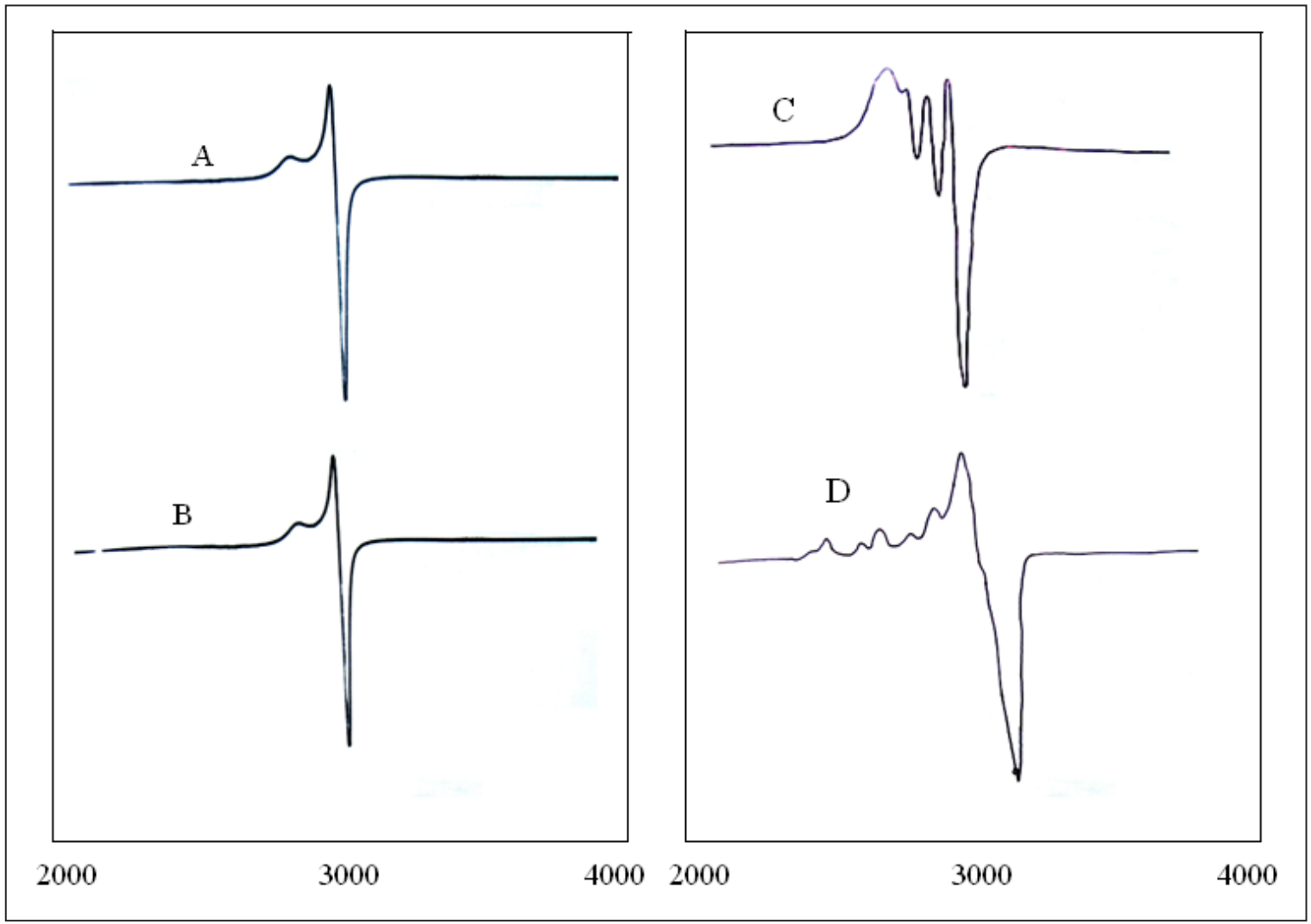

Fig 6.2.5: ESR spectra of $Cu_2(CH_3COO)_2(HAPHPMN)_2$ (A) in powder state at 300K, (B) at LNT, (C) in DMF solution at 300K and (D) at liquid nitrogen temperature

Based on molar conductance, magnetic moment, GC-MS, electronic, FT-IR and ESR spectral data the following structure **(Fig 6.2.6)** is suggested to the copper(II) and nickel(II) complexes of Schiff base ligands having polymethylene backbone. The complexes are supposed to have square planar geometry around the metal ion. In DMF medium the complexes may exhibit hexa coordination as the solvent molecules might have coordinated to metal ions.

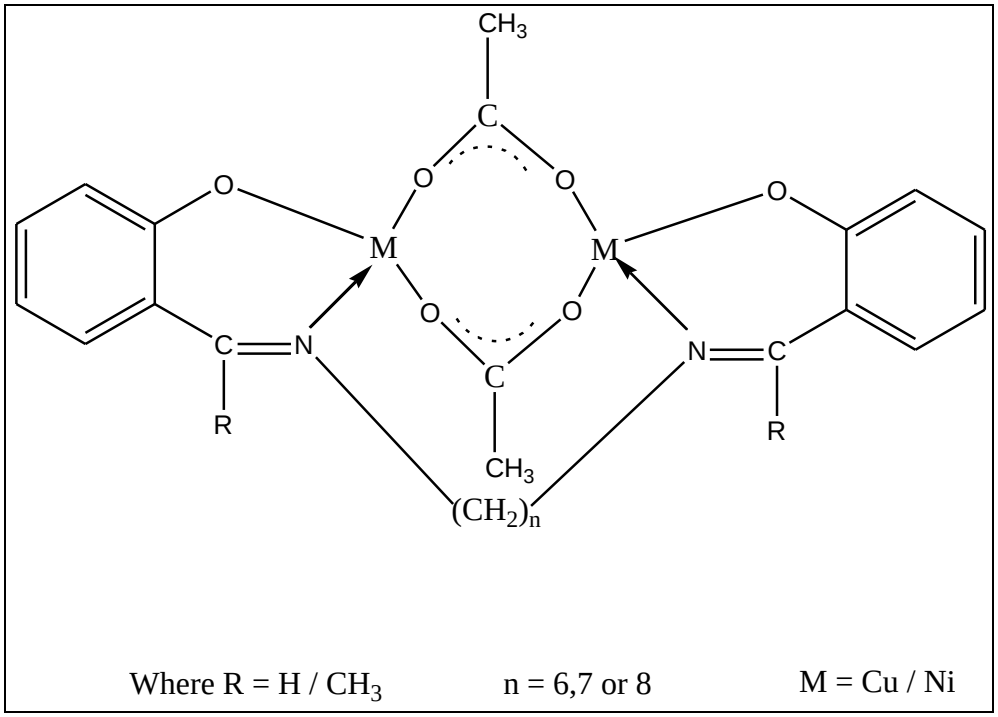

Fig 6.2.6: Tentative structure of the acetato bridged dinuclear metal complex

(g) Electrochemical studies:

Redox behavior of the copper (II) and nickel (II) complexes has been investigated by cyclic voltammetry in DMF using 0.1M tetrabutylammoniumhexaflourophosphate (TBAHEP) as supporting electrolyte. The cyclic voltammetric profile of $Cu_2(CH_3COO)_2(HAPHPMN)_2$ is given in **Fig 6.2.7**. The electrochemical data of copper(II) and nickel(II) complexes are presented in **Table 6.2.6.**

Repeated scans at various scan rates suggest that the presence of stable redox species in solution. $E_{1/2}$ values of all complexes observed at potential range of 0.808 – 0.849 V vs. Ag/AgCl [26-28]. It may be inferred that all the Cu (II) complexes undergo reduction to their respective Cu (I) complexes. The non-equivalent current in cathodic and anodic peaks (i_c/i_a= 0.205 and 1.44 at 100 mVs^{-1}) for complexes indicate quasi-reversible behavior [29]. The difference $\Delta E_p = E_{pc} - E_{pa}$ in all the complexes exceeds the Nerstian requirement 59/n mV (n= number of electrons involved in oxidation reduction) which suggests quasi-reversible character associated with a considerable reorganization of the coordination sphere during electron transfer [30]. The complexes have large separation (145-191 mV) between anodic and cathodic peaks indicating quasi-reversible character of redox reaction. The $E_{1/2}$ values of copper complexes are inversely related to the size of the complex [31]. From copper(II) complexes of SALOCMN to SALHXMN the $E_{1/2}$ values decrease gradually. Similarly from HAPOCMN to HAPHXMN copper(II) complexes, the same trend is exhibited. Complexes (I, III, V) derived from salicylaldehyde have high $E_{1/2}$ values when compared with complexes derived from o-hydroxyacetophenone.

The cyclic voltammograms of the nickel complexes showed two active responds in DMF in potential range -1.151 to -1.468 V vs. Ag/AgCl assigned to Ni^{II}/Ni^{III} couple and the values in potential range from -1.341 to -1.632 V vs. Ag/AgCl assigned to Ni^{II}/Ni^{I} couple.

The occurrence of such irreversible responses was observed in tetradentate Schiff base complexes of Ni (II) [32].

Comparison of the $E_{1/2}$ values of present copper(II) complexes with analogous nickel(II) complexes reveals that the copper complexes undergo more facile redox change which seems to be a requirement to the DNA cleavage [33-35]. DNA cleavage studies of the present complexes proved that copper complexes have positive $E_{1/2}$ values exhibit more activity than those of nickel complexes which have least activity towards DNA.

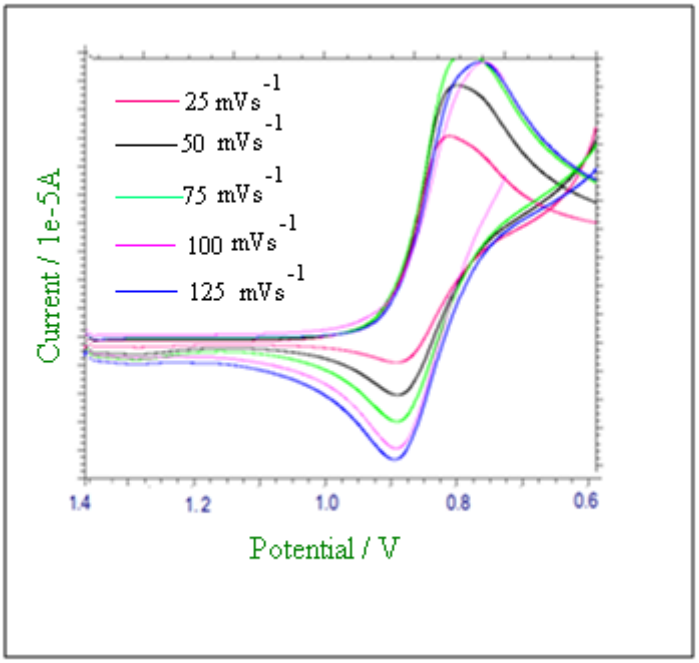

Fig 6.2.7: cyclic voltammetric profile of $Cu_2(CH_3COO)_2(HAPHPMN)_2$ at different scan rates 25, 50, 75, 100 and 125 mVs^{-1}

Table 6.2.6: Cyclic voltammetric data of copper (II) and Nickel (II) complexes

Complex	Redox couple	E_{pc} V	E_{pa} V	ΔE_p (mV)	$E_{1/2}$	$-i_c/i_a$	log K_c [a]	$-\Delta G^o$ [b]
$Cu_2(CH_3COO)_2(SALOCMN)_2$	II/I	0.730	0.886	156	0.808	0.224	0.214	1229
$Ni_2(CH_3COO)_2(SALOCMN)_2$	III/II	-1.372	-1.221	151	-1.296	-	0.222	1277
	II/I	-1.583	-1.391	192	-1.487	-	0.175	1004
$Cu_2(CH_3COO)_2(SALHPMN)_2$	II/I	0.731	0.912	181	0.821	0.327	0.184	1060
$Ni_2(CH_3COO)_2(SALHPMN)_2$	III/II	-1.448	-1.265	183	1.356	-	0.183	1054
	II/I	-1.556	-1.423	133	-1.489	-	0.252	1450
$Cu_2(CH_3COO)_2(SALHXMN)_2$	II/I	0.754	0.945	191	0.849	1.44	0.175	1004
$Ni_2(CH_3COO)_2(SALHXMN)_2$	III/II	-1.564	-1.322	242	-1.443	-	0.138	797
	II/I	-1.638	-1.465	173	-1.551	-	0.194	1115
$Cu_2(CH_3COO)_2(HAPOCMN)_2$	II/I	0.733	0.888	145	0.810	0.450	0.216	1244
$Ni_2(CH_3COO)_2(HAPOCMN)_2$	III/II	-1.260	-1.151	109	-1.205	-	0.308	1768
	II/I	-1.472	-1.341	131	-1.406	-	0.256	1472
$Cu_2(CH_3COO)_2(HAPHPMN)_2$	II/I	0.743	0.890	147	0.816	0.385	0.228	1312
$Ni_2(CH_3COO)_2(HAPHPMN)_2$	III/II	-1.426	-1.273	153	-1.349	-	0.219	1260
	II/I	-1.620	-1.493	127	-1.556	-	0.264	1518
$Cu_2(CH_3COO)_2(HAPHXMN)_2$	II/I	0.760	0.908	148	0.834	0.205	0.227	1303
$Ni_2(CH_3COO)_2(HAPHXMN)_2$	III/II	-1.468	-1.326	142	-1.397	-	0.236	1354
	II/I	-1.632	-1.511	121	-1.571	-	0.277	1594

[a] $\log K_c = 0.434\ ZF/RT\Delta E_p$; [b] $\Delta G^o = -2.303\ RT \log K_c$

h. DNA binding studies of copper and nickel complexes

The interaction of metal complexes was monitored by UV-visible spectroscopy. The absorption spectra of complexes were compared in the absence and in the presence of CT-DNA. In the presence of increasing amounts of DNA, the spectra of all complexes showed a strong decrease (Hypochromicity) or increase (Hyperchromicity) in intensity with shift in absorption maxima towards lower (blue-shift) or higher (red-shift) wave lengths. The change in absorbance values with increasing amount of CT-DNA were used to evaluate the intrinsic binding constant K_b for the complex.

Copper(II) complexes exhibit an intense absorption band around 275-385 nm whereas nickel(II) complexes exhibit an intense absorption band around 322-407 nm which is attributed to a π-π^* transitions. Absorption spectra were recorded in the range of 250-600 nm. Electronic absorption spectral data upon addition of CT-DNA and binding constants of these complexes are given in the **Table 6.2.7**. The change in absorbance values with increasing amounts of CT-DNA was used to evaluate the intrinsic binding constant K_b, for the complexes. In the presence of increasing amounts of CT-DNA, the UV-Visible absorption spectra of copper (II) complexes show bathochromic shift (λ_{max}: 2-7 nm) whereas those of the nickel (II) complexes show (λ_{max}: 1-12 nm). From the table it is also evident that nickel (II) complexes show hyperchromism. It is also evident that all the complexes bind with DNA with high affinities and, the estimated binding constants are in the range of 10^4 to 10^5 M^{-1}. This may be due to the presence of pi- stacking of the phenyl ring present in the Schiff base ligands. Typical absorption spectra of $Cu_2(CH_3COO)_2(HAPOCMN)_2$ are shown in **Fig.6.2.8**.

The binding constants (K_b) for DNA interaction of the complexes have been calculated by using the following equation:

$$[DNA] / (\varepsilon_a-\varepsilon_f) = [DNA] / (\varepsilon_b-\varepsilon_f) + 1/ K_b (\varepsilon_b-\varepsilon_f) \qquad (1)$$

Table 6.2.7:

Electronic absorption data upon addition of CT-DNA to Cu(II) & Ni(II) complexes

Complex	$\lambda_{max/nm}$		$\Delta\lambda$/nm	H%	$K_b(M^{-1})$
	Free	Bound			
$Cu_2(CH_3COO)_2(SALOCMN)_2$	368	361	7	15.23	2.03×10^5
$Ni_2(CH_3COO)_2(SALOCMN)_2$	384	372	12	62.23	1.28×10^4
$Cu_2(CH_3COO)_2(SALHPMN)_2$	352	349	3	27.22	3.12×10^5
$Ni_2(CH_3COO)_2(SALHPMN)_2$	346	345	1	15.26	1.63×10^4
$Cu_2(CH_3COO)_2(SALHXMN)_2$	325	327	2	32.45	4.04×10^5
$Ni_2(CH_3COO)_2(SALHXMN)_2$	334	330	3	26.47	5.55×10^4
$Cu_2(CH_3COO)_2(HAPOCMN)_2$	371	367	4	12.17	1.12×10^5
$Ni_2(CH_3COO)_2(HAPOCMN)_2$	404	407	3	33.63	1.10×10^4
$Cu_2(CH_3COO)_2(HAPHPMN)_2$	321	323	2	-2.93	1.25×10^5
$Ni_2(CH_3COO)_2(HAPHPMN)_2$	382	385	3	10.23	1.18×10^4
$Cu_2(CH_3COO)_2(HAPHXMN)_2$	278	275	3	9.27	2.02×10^5
$Ni_2(CH_3COO)_2(HAPHXMN)_2$	327	322	5	-6.71	1.26×10^4

From the **Table 6.2.7,** it is evident that the binding constants complexes are inversely related to the size of complex (or molecular weights). Complexes derived from the ligand SALHXMN exhibit higher binding constants whereas the complexes derived from the ligand HAPOCMN show lower affinity towards DNA. The order of binding affinities of copper complexes can be written as:

$Cu_2(CH_3COO)_2(SALHXMN)_2$ > $Cu_2(CH_3COO)_2(SALHPMN)_2$ >

$Cu_2(CH_3COO)_2(SALOCMN)_2$ > $Cu_2(CH_3COO)_2(HAPHXMN)_2$ >

$Cu_2(CH_3COO)_2(HAPHPMN)_2$ > $Cu_2(CH_3COO)_2(HAPOCMN)_2$.

This may be due to the steric hindrance effect of bulky groups present in the ligand portion of the complexes. Nickel complexes also follow the same trend. It is also evident that copper complexes have more affinity towards DNA than nickel complexes.

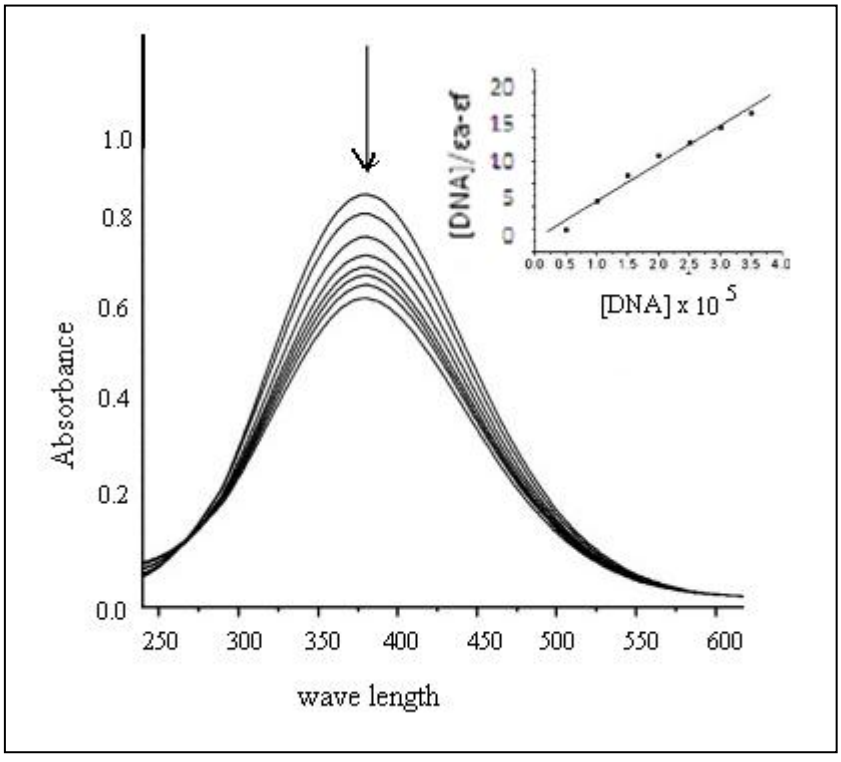

Fig 6.2.8:
Absorption spectra of $Cu_2(CH_3COO)_2(HAPOCMN)_2$ in the absence and in the presence of increasing concentration of CT-DNA. Uppermost curve stands for the absorption spectrum drawn in the absence of DNA. A plot of [DNA]/(ε_a-ε_f) versus [DNA] is shown in the inset

i. DNA cleavage activities of copper(II) and nickel(II) complexes

Nuclease activity of Schiff base ligands having long chain back bone and their copper (II) and nickel (II) complexes has been investigated using pBR 322 DNA by agarose gel electrophoresis in the presence and in the absence of H_2O_2 at 30 minutes incubation period [36,37]. At micromolar concentration, the ligands exhibit no significant activity in the absence or in the presence of the oxidant as shown in **Fig 6.2.9**. But the metal complexes show enhanced nuclease activity due to the presence of metal ions.

The nuclease activity of the copper complexes was also investigated in the presence of a free radical scavenger, dimethyl sulfoxide (DMSO), a chelating agent EDTA and a reducing agent dithiotreitol (DTT). Copper(II) complexes derived from salicylaldehyde/o-hydroxyacetophenone and 1,8-diaminooctane exhibit least nuclease activity when compared with other ligands. This may be due to their lesser redox potential values or the bulky size of the ligands. However, the nuclease activity is enhanced in presence of an oxidizing agent. The role of other reagents is nominal as they could not enhance or decrease the nuclease activity of these complexes. Nuclease activity of copper(II) complexes is shown in **Fig 6.2.10, Fig 6.2.11** and **Fig 6.2.12.**

As expected the nuclease activity of nickel complexes is found to be less when compared with those of copper complexes in the absence or in the presence of an oxidant H_2O_2 (**Fig 6.2.13**). The nuclease activity depends on the nature of metal ion. Comparatively higher nuclease activity of copper(II) complexes may be due to their favourable redox potential values (Cu (II)/Cu(I) from +0.808 to + 0.849 V). $E_{1/2}$ values of nickel complexes are found to be in the range -1.205 to -1.71 V.

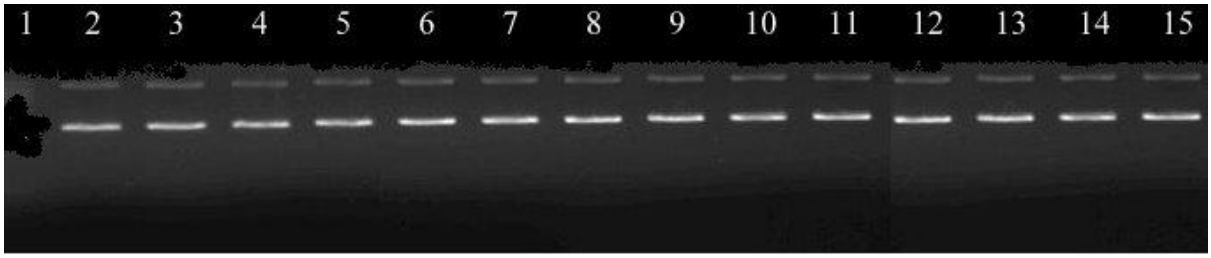

Fig 6.2.9: Agarose gel (0.8%) showing results of electrophoresis of 1µl of pBR 322 Plasmid DNA; 4µl of Tris-HCl/NaCl (50mM/5mM) buffer (pH-7); 2µl of complex ligand in DMF($1x10^{-3}$M); 11µl of sterilized water; 2µl of H_2O_2 (total volume 20µl) were added, respectively, incubated at 37^0C (30 min);

Lane 1: 1 kb DNA Ladder; Lane 2: DNA control; Lane 3: DNA control+ H_2O_2; Lane 4: SALOCMN + DNA; Lane 5: SALOCMN + DNA+ H_2O_2; Lane 6: SALHPMN + DNA; Lane7: SALHPMN + DNA+ H_2O_2; Lane8: SALHXMN + DNA; Lane 9: SALHXMN + DNA+ H_2O_2; Lane 10: HAPOCMN + DNA; Lane 11: HAPOCMN + DNA + H_2O_2 ; Lane 12: HAPHPMN + DNA; Lane 13: HAPHPMN + DNA + H_2O_2 ; Lane 14: HAPHXMN + DNA; Lane 15: HAPHXMN + DNA + H_2O_2 ;

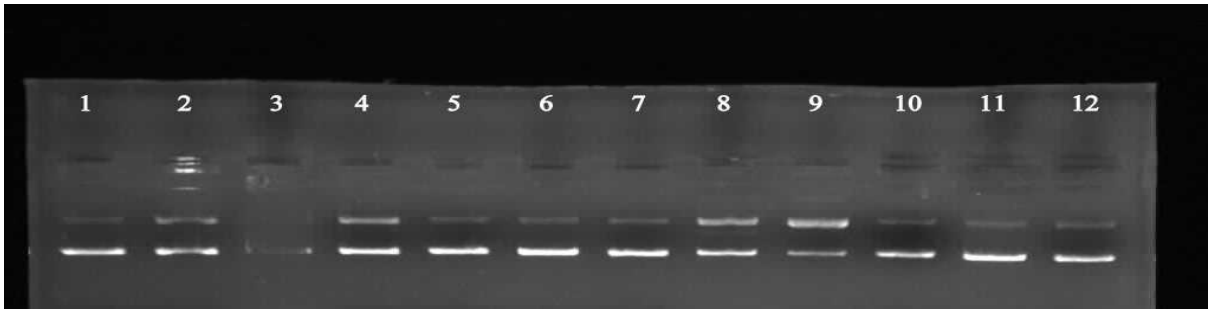

Fig 6.2.10: Agarose gel (0.8%) showing results of electrophoresis of 1µl of pBR 322 Plasmid DNA; 4µl of Tris-HCl/NaCl (50mM/5mM) buffer (pH-7); 2µl of complex in DMF($1x10^{-3}$M); 11µl of sterilized water; 2µl of H_2O_2 (total volume 20µl) were added, respectively, incubated at 37^0C (30 min);

Lane 1: DNA control; Lane 2: DNA control+ H_2O_2; Lane 3: $Cu_2(CH_3COO)_2(SALOCMN)_2$ + DNA; Lane 4: $Cu_2(CH_3COO)_2(SALOCMN)_2$ + DNA+ H_2O_2; Lane 5: $Cu_2(CH_3COO)_2(SALOCMN)_2$ + DNA+DMSO; Lane 6: $Cu_2(CH_3COO)_2(SALOCMN)_2$ + DNA+ EDTA; Lane 7: $Cu_2(CH_3COO)_2(SALOCMN)_2$ + DNA+DTT; Lane 8: $Cu_2(CH_3COO)_2(HAPOCMN)_2$ + DNA; Lane 9: $Cu_2(CH_3COO)_2(HAPOCMN)_2$+ DNA+ H_2O_2; Lane 10: $Cu_2(CH_3COO)_2(HAPOCMN)_2$+ DNA+DMSO; Lane 11: $Cu_2(CH_3COO)_2(HAPOCMN)_2$+ DNA+ EDTA; Lane 12: $Cu_2(CH_3COO)_2(HAPOCMN)_2$ + DNA+DTT;

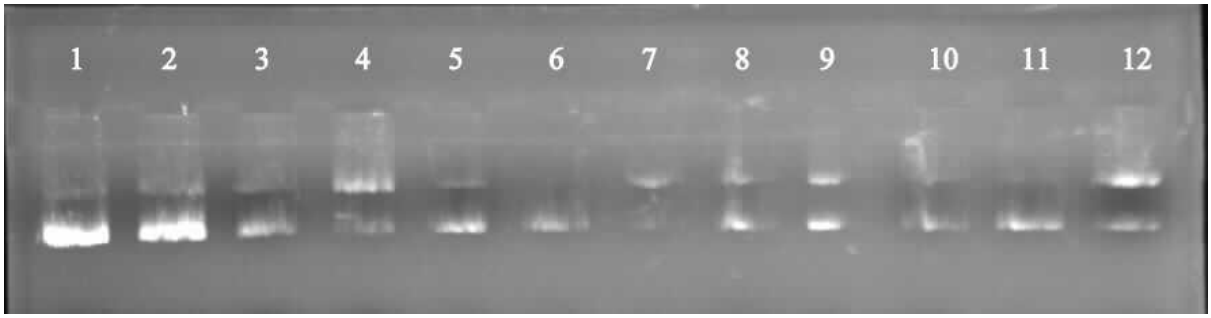

Fig 6.2.11: Agarose gel (0.8%) showing results of electrophoresis of 1µl of pBR 322 Plasmid DNA; 4µl of Tris-HCl/NaCl (50mM/5mM) buffer (pH-7); 2µl of complex in DMF($1x10^{-3}$M); 11µl of sterilized water; 2µl of H_2O_2 (total volume 20µl) were added, respectively, incubated at 37^0C (30 min);

Lane 1: DNA control; Lane 2: DNA control+ H_2O_2; Lane 3: $Cu_2(CH_3COO)_2(SALHPMN)_2$ + DNA; Lane 4: $Cu_2(CH_3COO)_2(SALHPMN)_2$ + DNA+ H_2O_2; Lane 5: $Cu_2(CH_3COO)_2(SALHPMN)_2$ + DNA+DMSO; Lane 6: $Cu_2(CH_3COO)_2(SALHPMN)_2$ + DNA+ EDTA; Lane 7: $Cu_2(CH_3COO)_2(SALHPMN)_2$ + DNA+DTT; Lane 8: Cu_2 $(CH_3COO)_2(HAPHPMN)_2$+ DNA; Lane 9: Cu_2 $(CH_3COO)_2(HAPHPMN)_2$+ DNA+ H_2O_2; Lane 10: Cu_2 $(CH_3COO)_2(HAPHPMN)_2$+ DNA+DMSO; Lane 11: Cu_2 $(CH_3COO)_2(HAPHPMN)_2$+ DNA+ EDTA; Lane 12: Cu_2 $(CH_3COO)_2(HAPHPMN)_2$+ DNA+DTT;

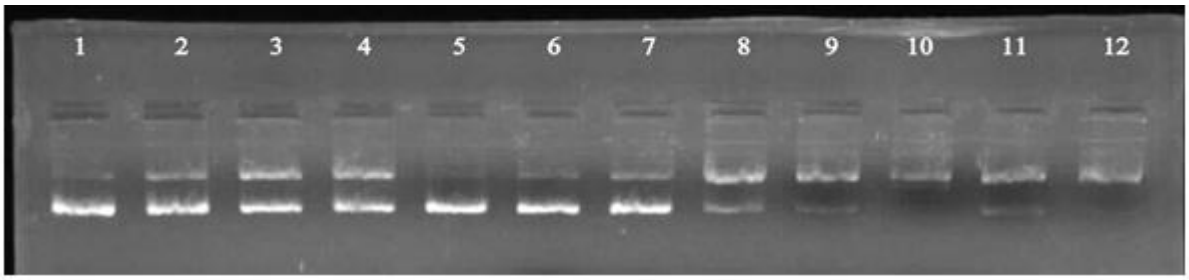

Fig 6.2.12: Agarose gel (0.8%) showing results of electrophoresis of 1µl of pBR 322 Plasmid DNA; 4µl of Tris-HCl/NaCl (50mM/5mM) buffer (pH-7); 2µl of complex in DMF($1x10^{-3}$M); 11µl of sterilized water; 2µl of H_2O_2 (total volume 20µl) were added, respectively, incubated at 37^0C (30 min);

Lane 1: DNA control; Lane 2: DNA control+ H_2O_2; Lane 3: $Cu_2(CH_3COO)_2(SALHXMN)_2$ + DNA; Lane 4: $Cu_2(CH_3COO)_2(SALHXMN)_2$ + DNA+ H_2O_2; Lane 5: $Cu_2(CH_3COO)_2(SALHXMN)_2$ + DNA+DMSO; Lane 6: $Cu_2(CH_3COO)_2(SALHXMN)_2$ + DNA+ EDTA; Lane 7: $Cu_2(CH_3COO)_2(SALHXMN)_2$ + DNA+DTT; Lane 8: $Cu_2(CH_3COO)_2(HAPHXMN)_2$ + DNA; Lane 9: $Cu_2(CH_3COO)_2(HAPHXMN)_2$ + DNA+ H_2O_2; Lane 10: $Cu_2(CH_3COO)_2(HAPHXMN)_2$ + DNA+DMSO; Lane 11: $Cu_2(CH_3COO)_2(HAPHXMN)_2$ + DNA+ EDTA; Lane 12: $Cu_2(CH_3COO)_2(HAPHXMN)_2$ + DNA+DTT;

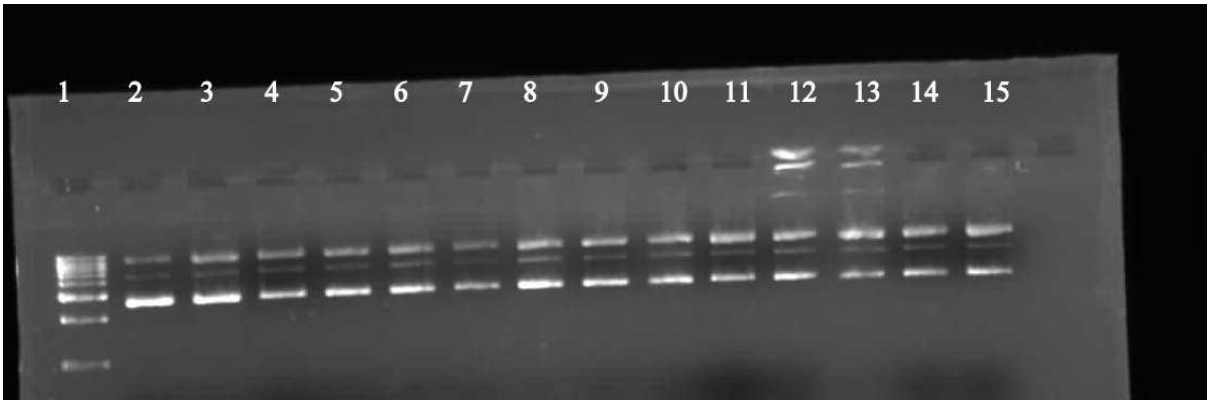

Fig 6.2.13: Agarose gel (0.8%) showing results of electrophoresis of 1µl of pBR 322 Plasmid DNA; 4µl of Tris-HCl/NaCl (50mM/5mM) buffer (pH-7); 2µl of complex in DMF($1x10^{-3}$M); 11µl of sterilized water; 2µl of H_2O_2 (total volume 20µl) were added, respectively, incubated at 37^0C (30 min);

Lane 1: 1 kb DNA Ladder; Lane 2: DNA control; Lane 3: DNA control+ H_2O_2; Lane 4: $Ni_2(CH_3COO)_2(SALOCMN)_2$ + DNA; Lane 5: $Ni_2(CH_3COO)_2(SALOCMN)_2$ + DNA+ H_2O_2; Lane 6: $Ni_2(CH_3COO)_2(SALHPMN)_2$ + DNA; Lane7: $Ni_2(CH_3COO)_2(SALHPMN)_2$ + DNA+ H_2O_2; Lane8: $Ni_2(CH_3COO)_2(SALHXMN)_2$ + DNA; Lane 9: $Ni_2(CH_3COO)_2(SALHXMN)_2$ + DNA+ H_2O_2; Lane 10: $Ni_2(CH_3COO)_2(HAPOCMN)_2$ + DNA; Lane 11: $Ni_2(CH_3COO)_2(HAPOCMN)_2$ + DNA + H_2O_2 ; Lane 12: $Ni_2(CH_3COO)_2(HAPHPMN)_2$ + DNA; Lane 13: $Ni_2(CH_3COO)_2(HAPHPMN)_2$ + DNA + H_2O_2 ; Lane 14: $Ni_2(CH_3COO)_2(HAPHXMN)_2$ + DNA; Lane 15: $Ni_2(CH_3COO)_2(HAPHXMN)_2$ + DNA + H_2O_2 ;

Conclusions:

Copper(II) and nickel(II) complexes of tetradentate Schiff base ligands incorporating salicylaldehyde/2-hydroxyacetophenone and polymethylene diamine backbone have been synthesized and characterized. Both copper(II) and nickel(II) complexes have square planar geometry in solid state. But in DMF medium the complexes are hexacoordinated due to axial coordination of solvent molecules. Copper(II) complexes bind with DNA very strongly when compared with nickel(II) complexes. This observation suggests that the complexes bind DNA via coordination of bases. Binding activity of metal complexes increases with decrease in the chain length. Copper(II) complexes exhibit DNA cleavage activity even in the absence of an oxidant, but this activity becomes more pronounced in the presence of an oxidant. The nuclease activity of nickel(II) complexes is found to be less when compared with those of copper(II) complexes in the absence or in the presence of an oxidant. High nuclease activity of copper(II) complexes may be attributed due to their favourable positive redox potential values.

References

1. Lin, H.; Feng, Y. L. *Chinese J. Struct. Chem*. 24(**2005**) 346–348
2. M.P. Weberski Junior, C.C. McLauchlan and C.G. Hamaker, *Polyhedron,* 25 (**2006)**, p. 119.
3. L. C. Nathan, J. E. Koehne, J. M. Gilmore, K. A. Hannibal, W. E. Dewhirst, and T. D. Mai , *Polyhedron,* 22**(2003)** 887-894.
4. R.G.Snyder, M.Maroncelli, H.L.Strauss, V.M.Hallmark, *J.Phys.Chem.* 90 **(1986)** 5623-5630.
5. K.Hussain Reddy, M.Surendra Babu, P.Suresh Babu, S.Dayananda, *Ind. J. Chem. Technol.,* 11 (**2004**) 29.
6. S. Anbu, M. Kandaswamy, *Polyhedron* 30 (**2011**) 123.
7. A.B.P. Lever, *"Inorganic Electronic Spectroscopy",* 2nd Edn. (Elsevier, Amsterdam) (**1984**).
8. K. Hussain Reddy, Y. Lingappa, *Trans. Met. Chem*., 19 (**1994**) 487.
9. S.K. Sahni, S.P.Gupta, S.K.Sangal and V.B. Rana, *J. Inorg. Nucl. Chem.*, 39, **1977**, 1098.
10. N.Tirumavalavan, S.Mariya Rayappan, P.Akilan, M.Kandaswamy, *Indian. J. Chem. Tech.* 11 (**2004**)29.
11. P.Haribabu, Y Patil , K Hussain Reddy & M Nethaji , *Trans. Met. Chem.*, 36 (8) (**2011**) 867.
12. M.Ibrahim, A.Nada, D.E.Kamal, *Indian Journal of Pure & Applied Physics*, 43 (**2005**) 911-917.
13. S.G.Teoh, G.Y .Yeap, C.C. Loh, L.W.Foong, B.Teo, H.K.Fun, *Polyhedron*, 16, (**1997)** 2213.
14. K.Nakamoto, *Infrared and Raman spectra of Inorganic and Coordination compounds,* (Wiley Interscience), New York., **1978.**
15. D.Kevelson and R.Neiman, *J. chem.Phys*, 35, (**1961**), 149.
16. N.Raman, A.Kulandaisamy, K.Jeyasubramanian., *Indian. J.Chem*., 41 A (**2002**) 942.
17. S.M. Mamdoush, S.M.Abou Elenein and H.M. Kamel., *Indian. J. Chem*, 41 A (**2002**) 297.
18. I.M.Procter, B.J. Hathaway and P.Nicholis, *J. Chem. Soc. Dalton Trans.,* (**1968**), 1678.

19. V. Philip, V.Sunil, M.R.P.Kurup, M.Nethaji, *Poyhedron*, 24 (**2005**), 1133.
20. B.Singh, B.P.Yadava and R.C.Agarwal, *Indian J. Chem.*, 23A, **1984**, 441.
21. B.J.Hathaway and A.A.G.Tomilson, *Coord. Chem. Rev*., 5 (**1970**), 1
22. A.H.Maki and B.R.McGarvery, *J. Chem.Phy*., 29 (**1958**) 31.
23. K.L. Reddy, S.Srihari and P.Lingaiah, *J.Indian Chem. Soc*., 61 (**1984**), 80.
24. B.J. Hathaway and D.E. Billing, *Coord. Chem. Rev*. 5(**1961**)143.
25. B.J.Hathaway, *Structure and Bonding*, 14 (**1971**) 49.
26. X.H. Bu, Z.H. Zhang, X. Cao, S. Ma and Y. Tichen. *Polyhedron* 16 (**1997**), p. 3525.
27. S Dhar, D Senapathi, PK Das, P Chattopadyay, M Nethaji, AR Chakravarthy, *J Am.Chem. Soc*, 125(**2003)**12218.
28. S.Djebbar-Sid , O.Benali-Baitich and J.P.Deloume, *Polyhedron*, 16**, (1997)** 2175.
29. A.A.Khumhar, S.B.Rendye, D.X. West, A.E.Libert, *tran. Met. Chem.*. 16, **(1991),** 276.
30. S.Usha, M.Palaniandavar., *J. chem. Soc., Dalton Trans*., (**1994**), 2277.
31. P.Muralikrishna, *Ph.D., thesis*, S.K.University, Anantapur, **2007.**
32. C. Santos, M. Vilas. Boas, M. F. M. Piedade, C. Freire, M. T. Duarte , B. De. Castro, *Polyhedron.*19 **(2000)** 655.
33. C.C.Cheng, S.E.Rokita and C.J.Burrows, *Angew. Chem., Int.Ed. Engl*., 32, (**1993)** 277.
34. J.G.Muller, X.Chen, A.C.Dadiz, S.E.Rokita and C.J.Burrows., *J.Am. Chem. Soc*., 114 **(1992),** 2407.
35. C.V. Sastri, D.Eswaramoorthy, L.Giribabu, B.G. Maiya., *J. Inorg. Biochem*., 94, (**2003**) 138.
36. P.Murali Krishna , K.Hussain Reddy , J.P. Pandey , S.Dayananda , *Trans. Met. Chem.* **(2008)** 33:661
37. P. Haribabu, Y. P. Patil, K Hussain Reddy, M. Nethaji, *Trans. Met. Chem.*36, 8 **(2011),** 867-874.